Title
THE K-pu> K| n-p REACTION FROM 1.0 TO 1.7 BeV/c

Author
Wojcicki, Stanley G.

Publication Date
1963-12-05

UCRL-11138

University of California

Ernest O. Lawrence Radiation Laboratory

THE $K^- p \rightarrow \bar{K}^0 \pi^- p$ REACTION FROM 1.0 TO 1.7 BeV/c

Berkeley, California

DISCLAIMER

submitted to Physical Review

UCRL-11138

UNIVERSITY OF CALIFORNIA
Lawrence Radiation Laboratory
Berkeley, California

AEC Contract No. W-7405-eng-48

THE $K^-p \rightarrow \bar{K}^0\pi^-p$ REACTION FROM 1.0 TO 1.7 BeV/c

Stanley G. Wojcicki

December 5, 1963

THE $K^-p \to \bar{K}^0\pi^-p$ REACTION FROM 1.0 TO 1.7 BeV/c*

Stanley G. Wojcicki†

Lawrence Radiation Laboratory
University of California
Berkeley, California

December 5, 1963

ABSTRACT

This report summarizes the study of the reaction $K^-p \to \bar{K}^0\pi^-p$ over the range of energies from 1.0 to 1.7 BeV/c. The reaction is shown to be dominated by the $K^{*-}p$ final state from threshold (1.08 BeV/c) to the highest energy available in this experiment. The best values for K^{*-} parameters are shown to be 891 and 46 MeV for the central value and full width of the resonance, respectively.

It is shown that the one-pion-exchange contribution dominates the low-momentum-transfer events at the higher energies. On the assumption that T=3/2 $K\pi$ interaction is negligible, which is strongly indicated by the data of Galtieri et al., the T=1/2 $K\pi$ S-wave phase shift is shown to be small and positive and roughly linear with the center-of-mass momentum in the $K\pi$ system. Influence of other unstable meson and baryon states on this reaction is discussed.

I. INTRODUCTION

The reaction $K^- p \rightarrow \bar{K}^0 \pi^- p$ provides a convenient process to study pion production by K^- mesons by using the bubble chamber technique. In this paper we present the results on the analysis of 5165 examples of this reaction in the energy range from 1.0 to 1.7 BeV/c. The reaction is dominated by the K^* production from threshold up to the highest energy accessible in this experiment.

Section II discusses briefly the details of the exposure and the data-analysis system used in the experiment. In sections III and IV we discuss the cross sections and the gross features of the reaction. Sections V and VI deal with the applicability of the one-pion exchange model to this reaction. Using the Chew-Low formalism, we obtain cross sections and phase shifts for the $K\pi$ scattering. Finally, the last section discusses the effect of the other final-state interactions upon the reaction in question.

II. EXPERIMENTAL METHOD

The experiment was performed by exposing the Lawrence Radiation Laboratory's 72-in. bubble chamber to a high-energy, 2-stage, separated K^- beam designed and built under the direction of H. K. Ticho.[1] The exposure lasted from September 1961 to June 1962. Altogether eight different momentum settings were used, ranging from 1.05 to 1.7 BeV/c. The lowest two (1.05 and 1.11) were obtained by tuning the beam for transmission of 1.22-BeV/c K mesons and then degrading them to the desired momentum by means of an uranium or copper absorber placed in front of the chamber. All other energies were obtained by tuning the magnets for the appropriate momentum. The typical momentum spread was ± 3 or 4%. The pion contamination was always less than 15%, and since it cannot contribute significantly to the topology under study, it does not concern us here. The typical K flux per picture

ranged from one at the lowest momentum to about 10 in some parts of the film at 1.70 BeV/c.

The events under study include only those in which $\bar{K}^0$ decayed in the chamber via the two-charged-pion mode. All of the film was scanned at least twice for that topology. A subsequent check of bona fide $\bar{K}^0 p\pi^-$ events indicated that they were missed less than 5% of the time on each scan. For three of the momenta--1.32, 1.42, and 1.51 BeV/c--part of the film was subsequently rescanned to reject those events that involved a sure Λ decay, in order to reduce the number of measurements required. It was verified that this procedure resulted in no loss of genuine $\bar{K}^0 p\pi^-$ events.

An IBM card was punched for each event found, and these in turn were converted into a magnetic-tape master list by using Alvarez Group library program LINGO. Under control of the LINGO program, cards were then generated for those events that one desired to have measured. These cards were used to control the measuring projector (Franckenstein) to the extent of stopping the film at the correct frame, centering the stage in the vicinity of the vertex, and entering the correct indicative information on paper tape. An operator recorded on this paper tape coordinates of several points on each track along with the appropriate reference points (fiducial marks) on the surface of the chamber glass. Typical measuring time for a V^0 2-prong event was of the order of 10 min.

After conversion of paper tape to magnetic tape, the data were processed through the IBM program PANAL. PANAL edited the data into a more compact format and also performed some basic checks. The PANAL output in turn served as the input to the spatial-reconstruction and kinematical-constraint program PACKAGE. The first part of PACKAGE reconstructed all tracks in space and calculated their curvatures, taking into account energy loss. Errors on all quantities were also calculated here. In the second part

of PACKAGE, kinematical fits were attempted to all hypotheses involving a Λ or K^0, two charged prongs, and one or no missing neutrals. The PACKAGE output was in the form of a binary tape which contained a summary of all attempted fits as well as the fitted quantities for those hypotheses that gave a successful fit. This tape served as the input to a FORTRAN language program EXAMIN, which decided on the basis of χ^2's for various hypotheses whether the event "passed" or not. In addition it also calculated quantities of interest for passing events. The EXAMIN program wrote a binary tape (data-summary tape) with this information (typically several hundred words, i.e., numbers per event) which was used to update a master data-summary tape (DST). This latter operation was performed under the control of the LINGO program in such a manner that events not on the master list or events that passed previously were rejected. Thus the DST was protected against having duplicate good measurements of the same event entered on it. The DST was then the master tape serving as the input to various FORTRAN programs which either summarized (eg. in form of histograms) the data as it was on the tape, or used these data to calculate new quantities. It should be mentioned that at each stage in this analysis system some BCD (printer tape) output was also generated to allow one to check the whole operation.[2]

The separation of the $\bar{K}^0 p\pi^-$ reaction from others of the same topology could ordinarily be achieved by reference to χ^2 only. Even at the highest momentum, the number of ambiguities was only of the order of 2%, and those could always be resolved by inspecting the ionization of the two positive tracks.

III. CROSS SECTIONS

The path length in this experiment was determined in the following manner:

a.) At the lower two momenta (1.05 and 1.11) all 3-prong events were measured, and thus an accurate count of τ decays was obtained. For all practical purposes, scanning efficiency for τ topology at these momenta was 100% because of relatively low energy of the beam and low track density.

b. At the higher momenta (P beam $\geq$ 1.22 BeV/c) two independent methods were used to obtain the path length. The first method involved counting all 3-prong events, and then correcting for scanning efficiency and 1-prong decays with a Dalitz pair. The second method was based on counting all interactions in approximately every tenth roll of film and then normalizing to the total film sample by the use of those interactions that were scanned for in all of the film (e.g., V^0 2 prongs). The path length was then obtained by referring to the counter measurements of the K^-p cross sections in this energy region.[3] The number of pion interactions was determined mainly from the number of observed double-V associated productions. At the highest momentum, where the pion contamination was the largest, this number was checked by counting the 2-prong interactions with energetic δ rays.

The data on the path length, as well as on the number of events observed at each momentum setting, is summarized in Table I. The size of the discrepancy between these two methods of obtaining path length gives us some idea of the absolute accuracy of these methods.

The cross sections for the reaction under study are displayed in Fig. 1. Above the K^* threshold, the cross section appears to stay reasonably constant, with a possible slight rise at the higher energies. To obtain the cross sections, we multiplied the raw data by 3 to allow for the K_2^0 and neutral decay modes of the $\bar{K}^0$, by about 1.06 for very short $\bar{K}^0$ (this number was

obtained by studying the lifetime curve of the $\bar{K}^0$) and by 1.0 to 1.25 at various momenta for events that failed to go through the system. A study of re-measurements at 1.22 and 1.51 BeV/c, where extensive second and third measurements were carried out on failing events, indicated that the absence of the events that fail on the first pass does not bias any of the distributions studied.

IV. GENERAL FEATURES OF THE REACTION

Except for the lowest momentum (1.05 BeV/c) all other momentum intervals under study lie above the K^* threshold. The opening up of this new channel is clearly seen in Fig. 1 as a sharp jump in the cross section in the vicinity of 1.08 BeV/c. The extent to which the K^* dominates our reaction can be seen from the mass plot of the $K\pi$ system (Fig. 2), as well as in the Dalitz plots of this reaction (Figs. 3 through 8). In the Dalitz plots we have divided the data into three momentum intervals--1.15 to 1.45 BeV/c, 1.45 to 1.55 BeV/c, and 1.55 to 1.7 BeV/c. Clearly, the K^* is just as dominant right above threshold (the lowest momentum interval) as it is at higher energies. To first order, there are no other effects (which would exhibit themselves as bands on the Dalitz plot) contributing to this reaction. In a subsequent section, we look into the question of secondary resonances in more detail, but for the purposes of this discussion it is clear that other effects do not seriously influence the study of K^* production and decay. The curve drawn over Fig. 2 represents a mixture of 75% K^* formation (represented by a Breit-Wigner curve with a central value of 891 MeV and Γ of 46 MeV) and 25% phase space. The fit is very good, and this 3:1 ratio seems to represent the data quite well at all energies in this experiment.

The higher-energy region in this experiment, $P_K > 1.45$ BeV/c, should give a fairly accurate central value and width of the K^*. Firstly, as

remarked previously, we observe no other strong effects in the reaction. Secondly, the K^* occurs roughly in the middle of phase space at those energies, and thus the kinematical factors do not influence the parameters in question.

The $K\pi$ mass spectrum in the vicinity of the K^* is displayed in Fig. 9 in 5-MeV intervals. The data were divided according to the incident momentum--those with $1.45 < P_K < 1.55$ BeV/c in Fig. 9a, and the ones with $1.55 < P_K < 1.75$ BeV/c in Fig. 9b. After subtraction of the estimated background (straight dashed line), the data were fitted with a Breit-Wigner curve with two parameters, the central value M^* and the full width Γ. Both subsets of data gave the best fit to identical values of these parameters, namely $M^* = 891 \pm 1$ MeV and $\Gamma = 46 \pm 3$ MeV.[4] The quoted errors are only statistical and do not include the uncertainties inherent in this procedure. The χ^2 for the fit using these parameters corresponds to a probability of 50 and 6% for the lower- and higher-momentum data, respectively.

V. ONE-PION EXCHANGE MODEL

In 1959 Chew and Low proposed a way to analyze experiments with virtual particles as targets (as for example pions in the cloud surrounding the nucleus).[5] They conjectured that the cross sections and scattering distributions for reactions of the type $\pi\pi \rightarrow \pi\pi$ or $\pi K \rightarrow \pi K$ could be obtained by measuring the two-dimensional distribution $\partial^2\sigma(\Delta^2, \omega^2)/\partial\omega^2\partial\Delta^2$, where ω is the mass of the $\pi\pi$ (or $K\pi$) system, and Δ^2 is the invariant four-momentum transfer squared given to the nucleon. More specifically, if applied to our reaction, the conjecture states that the distribution in question, $\partial^2\sigma(\Delta^2, \omega^2)/\partial\omega^2\partial\Delta^2$ when extended to the nonphysical values of Δ^2, will have a pole at the value $\Delta^2 = -\mu^2$ where μ is the mass of the exchanged particle--π^0 in this case--and the residue at this pole is related to the πK cross section at that value of ω^2. Quantitively, if applied to this reaction we have

$$\frac{\partial^2\sigma}{\partial\omega^2\partial\Delta^2} \xrightarrow[\Delta^2\to-\mu^2]{} \frac{f^2}{2\pi}\,\frac{\Delta^2/\mu^2}{(\Delta^2+\mu^2)^2}\,\frac{\left[\frac{1}{4}\omega^4-\frac{1}{2}\omega^2(\mu_1^2+\mu_2^2)+\frac{1}{4}(\mu_1^2-\mu_2^2)^2\right]}{q_{1L}^2}\,\sigma_{K\pi}(\omega),$$

where μ_1 is the mass of the incident particle (K^-), μ_2 the mass of the target particle (π^0), q_{1L} the laboratory momentum of the K meson, and f^2 the pion-nucleon coupling constant equal to 0.08. In other words, we postulate that one-pion exchange (Fig. 10) must dominate the reaction at $\Delta^2 = -\mu^2$. The same general statements can be made about the three-dimensional distribution $\partial^2\sigma(\omega^2, \Delta^2, \cos\theta)/\partial\omega^2\partial\Delta^2\partial\cos\theta$, where θ is the angle between the incident K^- and outgoing $\bar{K}^0$ as defined in the $\bar{K}^0\pi^-$ barycentric system. Thus the $K\pi$ scattering distribution can be obtained in a similar method by the total cross section by extrapolating this three-dimensional distribution to the pole.

In practice, the extrapolation experiments have proved to be very difficult since very large amounts of data at very low momentum transfers are required to make the extrapolation reliable.[6] On the other hand, the one-pion-exchange mechanism may dominate the physical region, so that extrapolation would not be necessary. The Chew-Low prescription then could be used to relate the laboratory quantities to the quantities in the $K\pi$ (or $\pi\pi$ system). Basically, this amounts to saying that just a linear term is sufficient in extrapolation.

The study of pion production by pions has indicated that at low-momentum transfers to the nucleon, reactions like $\pi+N \to \pi+\pi+N$ can be interpreted as the interaction of the incident pion with one of the pions in the cloud surrounding the nucleon, i. e. pion-pion scattering.[7] Even though detailed investigations of this phenomenon have shown that other mechanisms also contribute,[8] it is clear that, at least at a semi-quantitative level, the one-pion-exchange (OPE) model gives a faithful representation of the low-momentum-transfer data in πN interactions.

There has been considerably less work on the mechanisms involved in pion production by K mesons. The OPE model appears remarkably successful in explaining the behavior of the reaction $K^+ + p \rightarrow K^{*0} + N^{*++}$ studied by Chinowsky et al.,[9] Kraemer et al.,[4] and Ferro-Luzzi et al.[10] On the other hand, in the three-body states arising from K^+p collisions, a much more important contribution appears to come from the ρ exchange.[10-13] This can be attributed at least partially to the fact that the OPE model cannot lead to an N^* along with a K meson, and N^* production appears to dominate the $K\pi N$ final states.

In this section we would like to discuss the data in light of the OPE model. Since, as mentioned before, the K^* appears to be the only strong final-state resonance, a priori we might expect this situation to favor study of the pion-exchange mechanism much more than in the case of K^+ interactions.

In the region of validity of the OPE model, the data must satisfy several conditions. Firstly, the recoil nucleon in general exhibits backward peaking. It is difficult to state this requirement quantitatively since, in general, the form factors at the two vertices on each side of the propagator have some Δ^2 dependence.

Secondly, there can be no correlation between the orientations of the particles forming vertex A and those forming vertex B (see Fig. 10). This observation was first made by Treiman and Yang and stems from the fact that the pion is spinless and thus can carry no orientation information from one vertex to another.[14] Quantitively the requirement can be stated that the distribution in angle ϕ must be isotropic, where ϕ is the angle between $\underset{\sim}{P}_{in} \times \underset{\sim}{P}_{out}$ and $\underset{\sim}{K}^0 \times \underset{\sim}{\pi}^-$ in the incident K^- rest frame. Here P_{in} and P_{out} refer to the momentum vectors of the target proton and the recoil proton, respectively.

Thirdly, the relative cross section for the production of the various possible charge states is no longer arbitrary, but represents the requirements of charge independence at both vertices. This point need not concern us further here, since we are studying only one charge state.

Fourthly, the scattering distributions for the $K\pi$ final state must be characteristic of the predominant angular-momentum state.

For this discussion we have divided the data into three momentum intervals--$1.15 < P_{K^-} < 1.45$ BeV/c, $1.45 < P_{K^-} < 1.55$ BeV/c and $1.55 < P_{K^-} < 1.75$ BeV/c. The Δ^2 distribution for each of these intervals as a function of the $K\pi$ mass is shown in Fig. 11. It is clear that the number of low-momentum protons increases as the energies of the incident K^- become greater. This is easy to understand since, as the energy increases, the physical region approaches the pole at $\Delta^2 = -\mu^2$.

The distribution in the Treiman-Yang angle for the low-momentum-transfer events for these three energy intervals is displayed in Fig. 12. Within each momentum interval we have divided the data according to the $K\pi$ mass spectrum into three bins--below, at, and above the K^* resonance. Low-momentum-transfer events are defined here as those with $\cos\theta_{K^-p} < -0.9$, -0.8, and -0.7 for the lowest, middle, and highest momentum bins, respectively. This cutoff was obtained by inspecting the variation of the distribution in the $K\pi$ scattering angle as a function of the production angle in the K^* mass band, $865 < M(K\pi) < 910$ MeV. Since at greater angles the $\cos^2\theta_{K\pi}$ term appears to vanish, the OPE diagram could not be dominant (at least for this mass interval). We conclude from these distributions that the data do not show any statistically significant departures from isotropy at the two higher energy intervals but are inconsistent with the OPE diagram at the lowest energy.

The $K\pi$ scattering-angle distributions at the two higher energies are shown in Figs. 13 and 14. Their general behavior is again consistent

with the peripheral mechanism, exhibiting an S-wave background with a strong P-wave, characteristic of K^* resonance in the middle mass bin. The scattering-angle distributions at the higher momentum transfers (not shown) agree with isotropy for all mass intervals. The data thus appear to be consistent with the statement the the OPE diagram dominates the reaction under study for low-momentum-transfer events above 1.45 BeV/c. Low momentum transfer here means $\cos\theta_{K^-p} < -0.8$ ($\Delta^2 \lesssim 9\, m_\pi^2$) at ~ 1.5 BeV/c, and $\cos\theta_{K^-p} < -0.7$ ($\Delta^2 \lesssim 14\, m_\pi^2$) at 1.65 BeV/c.

VI. Kπ CROSS SECTIONS AND PHASE SHIFTS

In the preceding section we have shown that the low-momentum-transfer data at the higher energies appear to be dominated by the OPE diagram. Here we would like to interpret these data along the lines suggested by Chew and Low to obtain Kπ cross sections and phase shifts in this energy region.

The cross section for the Kπ scattering obtained by using the Chew-Low prescription is shown in Fig. 15. The dashed curve indicates the behavior of a resonant T=1/2 P-wave cross section for a reaction $K^-\pi^0 \to \bar{K}^0\pi^-$. The factor of 2/9 arises from Clebsch-Gordan coefficients. That the numbers came out quite reasonable gives us an added assurance of the validity of our procedure.

To arrive at numbers for the phase shifts, we must make certain basic assumptions as to the behavior of Kπ system. First, we assume that the phase shifts are real, i.e., there is no appreciable absorption in Kπ collisions. This assumption is probably quite good in view of a much lower cross section for double-pion production by K mesons in this energy region and a very low $K^* \to K\pi\pi$ decay rate.[15] Second, we assume that the only partial waves that contribute significantly are S waves in the T=1/2 and T=3/2 states, and a T=1/2 P wave. Then, under these assumptions the angular

distribution for the process $K^-\pi^0 \to \bar{K}^0\pi^-$ is given by

$$\frac{d\sigma}{d\Omega} = \lambda^2 \left\{ \frac{2}{9} \left[\sin^2\delta_0^1 + \sin^2\delta_0^3 + 2\sin\delta_0^1 \sin\delta_0^3 \cos(\delta_0^1 - \delta_0^3) \right] \right.$$

$$\left. + \frac{4}{3} \left[\sin\delta_0^1 \sin\delta_1^1 \cos(\delta_0^1 - \delta_1^1) + \sin\delta_1^1 \sin\delta_0^3 \cos(\delta_1^1 - \delta_0^3) \right] \cos\theta + 2\sin^2\delta_1^1 \cos^2\theta \right\},$$

where λ is the reduced K^- wavelength in the $K\pi$ system, and the phase shifts are denoted by δ_J^{2T}.

The scattering distributions for the $K\pi$ system are illustrated in Figs. 13 and 14. The curves are a fit to the data up to and including the quadratic term in $\cos\theta$ and appear to represent the data quite well. However, because of the small number of events, we cannot construe this as a very strong argument against D waves. The coefficients of the power series

$$\frac{d\sigma}{d\Omega} = \lambda^2 \sum_{n=0}^{2} A_n \cos^n\theta$$

resulting from this fit are given in Tables II and III. The general behavior of the data appears consistent with a dominant P wave at the resonance and a reasonably constant S-wave background.

In principle, one could fit the phase-shift expansion to the data and get the phase-shift solutions by the method of least squares. However, we feel that systematic errors would be introduced in this manner because of additional small mechanisms (besides the OPE) contributing to the reaction even at low momentum transfers. Thus, for example, ρ (or ω) exchange leading to K^* formation would result in a $\sin^2\theta_{K\pi}$ distribution, as opposed to $\cos^2\theta_{K\pi}$ for the OPE model.[16] This would have the effect of reducing the P-wave phase shift and increasing the S-wave contribution.

We feel that the following approach is more satisfactory. We take the P-wave phase shift to be determined from the parameters of the K^* resonance

and a proper behavior at low energies. The shape of the K^* resonance is assumed to follow a Breit-Wigner curve modified by λ^2=down to ≈ 815 MeV, where it joins smoothly with a q^4 curve, which is the required behavior for a P-wave scattering cross section. The point at 815 MeV was chosen because at that point the two curves have roughly the same slope. On the high-energy side we feel that the Breit-Wigner curve should give a reliable estimate of the P-wave cross-section curve up to about 960 MeV, i.e., ≈ $3\Gamma/2$, but beyond that extension of the curve would not be justified. Accordingly we shall not use the last mass bin, especially since above that mass value, D waves might become appreciable, and the momentum transfer involved also becomes larger.

Having obtained a P-wave phase shift in this manner (Fig. 16a), we can calculate a T=1/2 or T=3/2 S-wave phase shift from the coefficient of the linear term in $\cos\theta$, if we assume that only one isotopic spin predominates. This method has the advantage that most other production mechanisms will be incoherent with a one-pion exchange leading to a $K\pi$ state in a P wave, and thus will not contribute to A_1.[16]

Next, we want to roughly estimate the magnitude of the T=3/2 $K\pi$ interaction. The study of the reaction $K^-n \to K^-\pi^-p$ by Galtieri et al. has shown that there appear to be no strong final-state effects in the $K^-\pi^-$ (pure T=3/2 state) system.[17] For purposes of comparison, we show in Fig. 17 the Δ^2 dependence of our reaction as well as of the reaction studied by Galtieri et al. Since we are interested primarily in the relative size of the S-wave interaction in the two isospin states, we have displayed only the events characterized by $M(K\pi) < 800$ MeV. We see a much more pronounced backward peaking of the proton in Fig. 17b, indicating that the peripheral mechanism plays a much stronger role in the reaction $K^-p \to \bar{K}^0\pi^-p$ than in the reaction $K^-n \to K^-\pi^-p$; i.e., the T=3/2 $K\pi$ interaction is relatively weak.

To estimate quantitatively the size of the T=3/2 Kπ interaction we treat the reaction $K^-n \to K^-\pi^-p$ in the same way as $K^-p \to \bar{K}^0\pi^-p$; i.e., we assume that all of the events with $\Delta^2 < 9$ are produced by the OPE mechanism. This assumption gives us a cross section of about 3 mb for the process $K^-\pi^- \to K^-\pi^-$ in the energy range up to 800 MeV. Putting in the factor of 2/9 arising from the Clebsch-Gordan coefficients, we conclude that out of the total cross section of 5 mb for the process $K^-\pi^0 \to \bar{K}^0\pi^-$, less than 0.7 mb is contributed by the T=3/2 state. Accordingly, in the following discussion we neglect the T=3/2 state and assume that only T=1/2 contributes significantly to the reaction. The coefficient of the linear term in $\cos\theta$ reduces then to $4/3 \sin\delta_0^1 \sin\delta_1^1 \cos(\delta_0^1 - \delta_1^1)$.

The phase shifts obtained under these assumptions are shown in Fig. 16b and 16c. It should be mentioned that this method involves a fourfold ambiguity. Firstly there is another solution in which the phase shifts are near 90 deg. Secondly, two more sets are obtained by adding 180 deg to these two solutions. The solutions near 90 deg can be excluded, since they require a much larger isotropic term than is consistent with the data for low Kπ mass values. We feel that the solutions shown in Fig. 16 have the most likely physical behavior.

For comparison purposes we also show in Fig. 16 the center-of-mass momentum, $P_{c.m.}$ in the Kπ system. It can be seen that the phase shifts appear to go roughly as $P_{c.m.}$ with the increasing energy. This is the behavior expected if the zero-effective-range approximation is valid. The scattering length a then turns out to be negative and roughly one-half of the K-meson Compton wavelength.

In principle, we could check our phase-shift assignments by comparing the measured A_0 and A_2 coefficients with the values that we would expect from the phase shifts obtained above. If we do this, we see that the measured A_0 is consistently higher than predicted, and A_2 is consistently lower. One possible

explanation of this behavior is that some ρ (or ω or ϕ) exchange contributes to the reaction even at the very low-momentum transfers. We should stress, however, that the ρ exchange (or its interference with π-exchange processes) cannot contribute to A_1 and thus does not invalidate our method.

In summary, we would like to emphasize that these results should be interpreted only in a semi-quantitative way. There are too many intrinsic difficulties and uncertainties to allow a completely quantitative argument. On the other hand, the fact that the answers do have reasonable physical behavior and that the $K\pi$ cross section at resonance has the correct magnitude leads us to believe that the overall procedure is reasonably valid.

VII. INFLUENCE OF OTHER STATES

It is clear from the Dalitz plots (Figs. 3 through 8) that no strong final-state interactions dominate the reaction under study other than the 891-MeV K^*. On the other hand, a weak contribution from other states would not readily exhibit itself on a Dalitz plot, especially in the presence of another, much stronger, resonance. In this section we examine the mass plots to study any possible enhancements due to other processes.

A. Pion-Nucleon Systems

The only pion-nucleon isobar accessible kinematically in the whole energy region under study is the 1238-MeV N^* (3, 3 resonance). The threshold for the production of 1512-MeV pion-nucleon resonance occurs at 1.5 BeV/c, and thus only in the highest energy region would we expect it to contribute to the reaction.

The analogous K^+p reaction, $K^+p \rightarrow K^0p\pi^+$, shows very strong $N^*(1238)$ production in the comparable energy region. Furthermore, study of production and decay angular correlations indicates that the dominant mechanism is ρ exchange.[10-13] Accordingly, from the pure isotopic-spin factor at the ρpN^* vertex,

we would expect a suppression of N^* production in our reaction by a factor of 9, if ρ exchange were also to dominate here. Indeed, we do observe an almost negligible contribution due to N^* production (Fig. 18a) of about 200 events, approximately a 4% effect. Elimination of K^* events does not seem to enhance the N^* (Fig. 18b). Needless to say, because of low signal-to-noise ratio, we can not say anything definite about the N^* production mechanism in this reaction. For the 1512-MeV resonance, even the highest energy interval does not show any statistically significant enhancement.

B. $\bar{K}^0p$ Systems

The only well-established T=1 resonance that can be produced in this energy region and subsequently decay into the $\bar{K}N$ system is the 1660-MeV hyperon. Previous work based in part on a fraction of the data presented here (approximately one-third of the total data at 1.51 BeV/c) indicated a very low branching ratio of the 1660-MeV isobar into the $\bar{K}N$ system ($\Gamma_{\bar{K}N}/\Gamma_{total} = x \approx 0.04$).[18] The experiment of Bastien and Berge was shown to be inconsistent with a value of x smaller than 0.16.[19] In appraising the significance of this discrepancy, we must remember the difficulties associated with studying a weakly produced resonance in the presence of a much stronger effect (K^* in this case). A small alignment of the K^* along its line of flight can alter considerably the expected $\bar{K}^0p$ mass spectrum.

Two additional experiments have recently indicated that the decay rate of $Y^*(1660)$ into the $\bar{K}N$ system is relatively low. Firstly, study of high energy π^-p interactions at Berkeley has given a value of approximately 0.2 for x.[20] Secondly, the work of Alston et al.[21] on the reactions $K^-n \to \Sigma^+\pi^-\pi^-$ $K^-n \to \Sigma^-\pi^+\pi^-$ indicates that the neutral component of $Y^*(1660)$ is produced by 1.5-BeV/c K mesons incident on neutrons. Furthermore, the data of Galtieri et al. can be used to obtain an upper limit on how many events in the reaction $K^-n \to K^-n^-p$ can be attributed to $Y^*(1660)$.[17] Combining the numbers

of Alston et al. with those of Galtieri et al., we obtain an upper limit of 1/8 on $\Gamma(\bar{K}N)/\Gamma(\Sigma\pi)$. Then, if we use the $Y^*(1660)$ branching ratio given by Alvarez et al.,[18] x turns out to be less than or equal to 0.04. Thus all indications are that the Y^* $\bar{K}N$ decay rate is quite low, although the exact value is still undetermined. Hence, considering the cross sections for $Y^*(1660)$ production in this energy region, we would not expect a large effect in the $\bar{K}^0p$ mass spectrum due to $Y^*(1660)$.

Galtieri et al. have recently observed an enhancement in the K^-p system at 1765 MeV.[17] Furthermore, they have shown that the existing K^-p and K^-n data in the region from 800 MeV/c to 1.15 BeV/c can be interpreted quite well, if one requires a T=1 assignment for this effect. Accordingly, it is of great interest to see if a similar effect is present in the $\bar{K}^0p$ system in our reaction. Assuming only production from the T=1 state, we would expect in our data an enhancement of about 150 events at 1.51 BeV/c. Of course, one could make this enhancement arbitrarily small by requiring the proper phase and magnitude for the production amplitudes from the T=0 and T=1 states.

The $\bar{K}^0p$ mass spectrum from all momenta under study is shown in Fig. 19a. There are no significant departures from the distribution expected if the sole contribution to this channel were 75% K^* production and 25% phase space.

On the other hand to see if there is any contribution from the above-mentioned $\bar{K}^0p$ resonant states we are justified in removing the events which would have a priori small possibility of showing any structure in the $\bar{K}^0p$ system. These would be the events in the K^* band as well as the low-momentum-transfer events, since the latter are most likely dominated by the $K\pi$ interaction (see the preceding discussion). Because the energy region under study lies not too far above the threshold for these two states under discussion, we would not expect a sharp backward peaking of the nucleon, even if K^* exchange were the dominant production mechanism.

The $\bar{K}^0p$ mass plot after subtraction of these two groups of events is shown in Fig. 19b. The curve again indicates the expected distribution if one takes into account the subtraction of K^* events. It is worth noting that the only positive departures from this curve are observed in the region of these two excited hyperons. The enhancement near 1780 MeV has a statistical significance of about three standard deviations if we remove the events with $P_K < 1.45$ BeV/c (shaded region), most of which lie below the threshold for the production of this state. We do not, however, believe that these data necessarily establish the existence of a T=1 resonance in this region, even if the effect is accepted as statistically significant. An examination of the Dalitz plot at 1.5 BeV/c (Fig. 5) shows an effect that could be interpreted as a constructive interference of the K^* with the N^*. That region of the Dalitz plot corresponds to the mass of the $\bar{K}^0p$ system in the vicinity of 1780 MeV. Thus an alternative interpretation of the effect is that we are merely seeing the projection of these events on the $\bar{K}^0p$ mass plot. Considering, however, the narrow width of this enhancement as well as the relatively large energy region in question (1.45 to 1.75 GeV/c), we feel that this latter hypothesis is less likely.

To summarize the discussion of the $\bar{K}^0p$ mass plots, we can clearly conclude that there are no strong contributions to this reaction from any $\bar{K}N$ excited state. We feel that the most logical explanation of the data is that there are small contributions to the reaction from both $Y_1^*(1660)$ and $Y_1^*(1765)$ productions amounting to approximately 2% and 1% of the total reaction, respectively. However, there are enough difficulties inherent in this analysis that we do not feel that the experiment can be said to establish the existence of a T=1 resonance near 1765 MeV.

C. Kappa Production

In a previous communication we have shown that the data require a narrow K-π resonance with a central value of 723 ± 3 MeV.[22] The final data presented here contribute little new information on this phenomenon, because the only new data added since the last report come from momenta of 1.6 and 1.7 BeV/c, where the cross section for κ production is negligible. Accordingly, we only briefly summarize the results. The lower part of the Kπ mass spectrum is shown in Figs. 20a through 20d, where the data are divided into the three momentum intervals-- $P_K < 1.45$ BeV/c, $1.45 < P_K < 1.55$ BeV/c, and $P_K > 1.55$ BeV/c. To obtain a quantative estimate of the κ cross section, we subtract from the three 5-MeV bins centered at 725 MeV the average of the six neighboring bins (three on each side). Assuming the T=1/2 assignment[17,23] and no appreciable radiative decay modes, we obtain 30, 20, and 15 μb for the cross section in the low, middle, and high momentum intervals. Obviously, these numbers should not be taken literally, but should serve merely as a rough indication of the size of the effect.

As shown previously, any systematic effects present are not large enough to contribute any appreciable broadening to the κ peak.[22] The experimental resolution in this mass region is of the order of 6 MeV(Γ_R = 6 MeV). We feel, however, that because of limited statistics, it would be dangerous to conclude that the width is finite and that the data exclude zero width.

ACKNOWLEDGMENTS

The author is deeply indebted to his many colleagues for their help and suggestions at all stages of this experiment. The continuing support, interest and encouragement of Professor Luis W. Alvarez is acknowledged with deep gratitude. The author would like to thank Drs. Margaret H. Alston and George R. Kalbfleisch, and Prof. Harold K. Ticho for their contributions in the early stages of this work and many helpful criticisms. The conversations with Dr. Robert Huff on the exchange models have been very helpful. Finally, special thanks are due to the members of the Bevatron and 72-inch bubble chamber crews, as well as to the Alvarez group measuring and scanning staff and programming staff, without whose support this work would have been impossible.

Table I. Data on path lengths and cross sections

K^- momentum (BeV/c)	No. of events (uncorrected)	Path length (events/mb) (from τ count)	Path length (events/mb) (from interaction count)	Cross section (mb)
1.05	56	141		0.78±0.11
1.11	71	216		1.51±0.20
1.215	577	1170	1275	1.49±0.12
1.32	587	1475	1385	1.44±0.12
1.42	406	800	810	1.81±0.15
1.505	2511	5090	5190	1.73±0.12
1.60	339	675	730	1.85±0.2
1.695	618	1065	1085	2.24±0.25

Table II. Coefficients of the power series $\sum_{n=0}^{2} A_n \cos^n\theta$ fitted to the data with $1.45 < P_K < 1.55$ BeV/c.

Mass interval (MeV)	A_0	A_1	A_2
638 to 800	0.03±0.01	0.01±0.01	-0.01±0.01
800 to 865	0.12±0.02	0.17±0.03	0.08±0.05
865 to 910	0.33±0.04	0.07±0.06	0.34±0.11
910 to 960	0.16±0.03	-0.10±0.06	0.08±0.08
960 to 1200	0.09±0.03	-0.12±0.04	0.20±0.08

Table III. Coefficients of the power series $\sum_{n=0}^{2} A_n \cos^n\theta$ fitted to the data with $1.55 < P_K < 1.75$ BeV/c.

Mass interval (MeV)	A_0	A_1	A_2
638 to 800	0.04±0.008	0.03±0.01	0.01±0.02
800 to 865	0.16±0.04	0.17±0.04	0.12±0.09
865 to 910	0.55±0.08	0.01±0.12	0.85±0.11
910 to 960	0.22±0.05	-0.14±0.07	0.18±0.14
960 to 1200	0.09±0.02	-0.10±0.03	0.11±0.07

FOOTNOTES AND REFERENCES

*This work was done under the auspices of the U. S. Atomic Energy Commission.

†Now at L' Ecole Polytechnique, Paris, France.

1. R. Hubbard, D. O. Huwe, G. Kalbfleisch, J. Kirz, D. Miller, J. B. Shafer, D. Stork, H. K. Ticho, and C. Wohl, Lawrence Radiation Laboratory Report UCRL-10690, 1964 (unpublished).
2. For a more complete description of the Alvarez group data-reduction system, see for example W. E. Humphrey and A. H. Rosenfeld, Analysis of Bubble Chamber Data, submitted to Annual Review of Nuclear Science (Annual Reviews, Inc., Palo Alto, California, 1963), Lawrence Radiation Laboratory Report UCRL-10812, June 17, 1963 (unpublished).
3. V. Cook, Bruce Cork, T. F. Hoang, D. Keefe, L. T. Kerth, W. A. Wenzel, and T. F. Zipf, Phys. Rev. 123, 320 (1961).
4. This central value should be compared to 892±2 MeV obtained for the neutral member of the K^* multiplet by R. Kraemer, L. Madansky, I. Miller, A. Pevsner, C. Richardson, R. Singh, and R. Zdanis, Proceedings of the Athens Topical Conference on Recently Discovered Resonant Particles (Ohio University, Athens, Ohio, 1963), p. 130.
5. G. F. Chew and F. E. Low, Phys. Rev. 113, 1640 (1959).
6. See for example L. B. Auerbach, T. Elioff, W. B. Johnson, J. Lach, C. E. Wiegand, and T. Ypsilantis, Phys. Rev. Letters 9, 173 (1962).
7. D. Carmony and R. Van de Walle, Phys. Rev. Letters 8, 73 (1962); V. Hagopian and W. Selove, Phys. Rev. Letters 10, 533 (1963); Z. G. T. Guiragossian, Phys. Rev. Letters 11, 85 (1963).
8. See for example E. Pickup, D. K. Robinson, and E. O. Salant, Phys. Rev. Letters 9, 170 (1962).

9. W. Chinowsky, G. Goldhaber, S. Goldhaber, W. Lee, and T. O' Halloran, Phys. Rev. Letters 9,330 (1962); also G. Goldhaber, Proceedings of the Athens Topical Conference on Recently Discovered Resonant Particles (Ohio University, Athens, Ohio, 1963) p. 80.

10. M. Ferro-Luzzi, R. George, Y. Goldschmidt-Clermont, V. P. Henri, B. Jongejans, D. Leith, G. Lynch, F. Muller, and J. M. Perreau; submitted to the 1963 Sienna International Conference on Elementary Particles.

11. S. Goldhaber, Proceedings of the Athens Topical Conference on Recently Discovered Resonant Particles (Ohio University, Athens, Ohio, 1963), p. 92.

12. B. Kehoe, Phys. Rev. Letters 11, 93 (1963).

13. G. B. Chadwick, D. J. Crennell, W. T. Davies, M. Derrick, J. H. Mulvey, P. B. Jones, D. Radojicic, C. A. Wilkinson, A. Bettini, M. Cresti, S. Limentani, L. Perusso, and R. Santangelo, Phys. Letters 6, 309 (1963).

14. S. B. Treiman and C. N. Yang, Phys. Rev. Letters 8, 140 (1962).

15. S. G. Wojcicki, M. H. Alston, and G. R. Kalbfleisch, Lawrence Radiation Laboratory Report UCRL-11139, December 1963, submitted to Physical Review.

16. See for example G. A. Smith, J. Schwartz, D. H. Miller, G. R. Kalbfleisch, R. W. Huff, O. I. Dahl, and G. Alexander, Phys. Rev. Letters 10, 138 (1963), and Robert W. Huff, Pseudoscalar and Vector Exchanges in the Production of Vector Mesons, Lawrence Radiation Laboratory Report UCRL-11003, September 5, 1963 (submitted to Physical Review).

17. A. Barbaro-Galtieri, A. Hussain, and R. D. Tripp, Phys. Letters 6, 296 (1963).

18. L. W. Alvarez, M. H. Alston, M. Ferro-Luzzi, D. O. Huwe, G. R. Kalbfleisch, D. H. Miller, J. J. Murray, A. H. Rosenfeld, J. B. Shafer, F. T. Solmitz, and S. G. Wojcicki, Phys. Rev. Letters 10, 184 (1963).

19. P. L. Bastien and J. P. Berge, Phys. Rev. Letters 10, 188 (1963).

20. Gerald A. Smith, Proceedings of the Athens Topical Conference on Recently Discovered Resonant Particles (Ohio University, Athens, Ohio, 1963), p. 67.

21. Margaret H. Alston, A. Barbaro-Galtieri, A. H. Rosenfeld, and S. G. Wojcicki, Lawrence Radiation Laboratory Report UCRL-11137, December 1963, to be submitted to Physical Review.

22. S. G. Wojcicki, G. R. Kalbfleisch, and M. H. Alston, Physics Letters 5, 283 (1963).

23. D. H. Miller, G. Alexander, O. I. Dahl, L. Jacobs, G. R. Kalbfleisch, and G. A. Smith, Physics Letters 5, 279 (1963).

FIGURE LEGENDS

Fig. 1. Cross section for the reaction $K^-p \to \bar{K}^0\pi^-p$ as a function of momentum. The low-energy points are from Bastien and Berge (Ref. 19) and Alston et al., Phys. Rev. Letters 6, 300 (1961).

Fig. 2. Mass spectrum of the $\bar{K}^0\pi^-$ system. The curve represents 75% K^* production ($M^* = 891$ MeV and $\Gamma = 46$ MeV) and 25% phase space.

Fig. 3. Dalitz plot for the reaction $K^-p \to \bar{K}^0p\pi^-$, for the events defined by $1.15 < P_{K^-} < 1.45$ BeV/c. The envelopes correspond to incoming momenta of 1.15 and 1.45 BeV/c.

Fig. 4. Same as 3.

Fig. 5. Dalitz plot for the reaction $K^-p \to \bar{K}^0p\pi^-$ for the events defined by $1.45 < P_{K^-} < 1.55$ BeV/c. The envelopes correspond to incoming momenta of 1.45 and 1.55 BeV/c.

Fig. 6. Same as 5.

Fig. 7. Dalitz plot for the reaction $K^-p \to \bar{K}^0p\pi^-$ for the events defined by $1.55 < P_{K^-} < 1.75$ BeV/c. The envelopes correspond to incoming momenta of 1.55 and 1.75 BeV/c.

Fig. 8. Same as 7.

Fig. 9. Mass spectrum of the $\bar{K}^0\pi^-$ system near the K^* region for events defined by (a) $1.45 < P_{K^-} < 1.55$ BeV/c, and (b) $1.55 < P_{K^-} < 1.75$ BeV/c. The straight dashed line represents our estimate of the background. The dashed curves represent a Breit-Wigner curve with $M^* = 891$ MeV and $\Gamma = 46$ MeV.

Fig. 10. One-pion-exchange Feynman diagram for the reaction $K^-p \to \bar{K}^0\pi^-p$.

Fig. 11. Scatter diagram of Δ^2 vs ω^2 for the reaction $K^-p \to \bar{K}^0\pi^-p$. The three parts of the figure are defined according to the incident momentum: (a) $1.15 < P_{K^-} < 1.45$ BeV/c, (b) $1.45 < P_{K^-} < 1.55$ BeV/c, and (c) $1.55 < P_{K^-} < 1.75$ BeV/c.

Fig. 12. Treiman-Yang angle for the low-momentum-transfer events.

Fig. 13. Distribution in the $K\pi$ scattering angle for the events with incident momenta between 1.45 and 1.55 BeV/c. (a) $M(K\pi) < 800$ MeV, (b) $800 < M(K\pi) < 865$ MeV, (c) $865 < M(K\pi) < 910$ MeV, (d) $910 < M(K\pi) < 960$ MeV, and (e) $M(K\pi) \gtrsim 960$ MeV.

Fig. 14. Distribution in the $K\pi$ scattering angle for events with incident momenta between 1.55 and 1.75 BeV/c. (a) $M(K\pi) < 800$ MeV, (b) $800 < M(K\pi) < 865$ MeV, (c) $865 < M(K\pi) < 910$ MeV, (d) $910 < M(K\pi) < 960$ MeV, and (e) $M(K\pi) \gtrsim 960$ MeV.

Fig. 15. Cross section for the reaction $K^-\pi^0 \to \bar{K}^0\pi^-$ obtained by using the Chew-Low prescription. (a) Events with $1.45 < P_{K^-} < 1.55$ BeV/c and (b) $1.55 < P_{K^-} < 1.75$ BeV/c.

Fig. 16. (a) Assumed T=1/2 P-wave phase shift for $K\pi$ scattering, (b) T=1/2 S-wave phase shift obtained by using the data with incident momenta between 1.45 and 1.55 BeV/c, and (c) T=1/2 S-wave phase shift obtained by using the data with incident momenta between 1.55 and 1.75 BeV/c. The dashed curve represents the c.m. momentum in the $K\pi$ system.

Fig. 17. The distribution in momentum transfer (Δ^2) for events with $M(K\pi) < 800$ MeV. In Fig. 17a we show the data of Galtieri et al. (Ref. 17) for the reaction $K^-n \to K^-\pi^-p$ at 1.5 BeV/c; in Fig. 17b are shown our data for the reaction $K^-p \to \bar{K}^0\pi^-p$ for the events with $1.45 < P_K < 1.55$ BeV/c.

Fig. 18. Mass spectrum of the $p\pi^-$ system for the reaction $K^-p \to \bar{K}^0\pi^-p$ from all energies in this experiment. Fig. 18a shows all the data; in Fig. 18b the events with $865 < M(K\pi) < 910$ MeV have been subtracted out. The curves show the phase-space predictions.

Fig. 19. Mass spectrum of the $\bar{K}^0 p$ system for the reaction $K^- p \rightarrow \bar{K}^0 \pi^- p$ from all energies in this experiment. Fig. 19a shows all the data; in Fig. 19b the events with $865 < M_{K\pi} < 910$ MeV and $\cos\theta_{K^-p} < -0.5$ have been subtracted out. The shaded region in Fig. 19b represents only those data with $P_K < 1.45$ BeV/c. The curves show the phase-space predictions. The lower curve in 19b is normalized to the data outside of the 1660 and 1780 MeV regions.

Fig. 20. Mass spectrum of the $\bar{K}^0 \pi^-$ system near the κ region. The four parts of the figure correspond to (a) $P_K < 1.15$ BeV/c, (b) $1.45 < P_K < 1.55$ BeV/c, (c) $P_K > 1.55$ BeV/c, and (d) data from all energies combined.

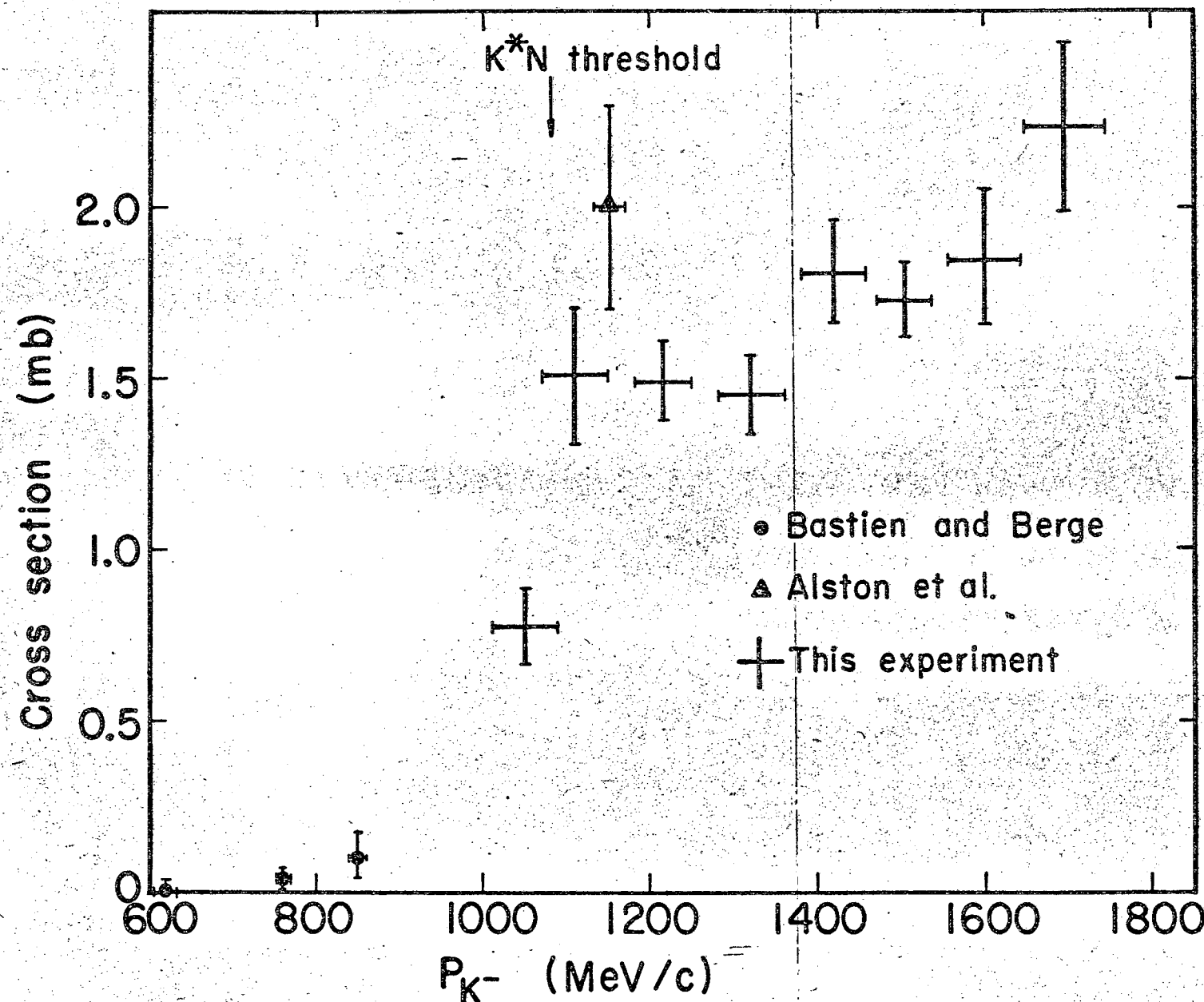

Fig. 1

MU-32834

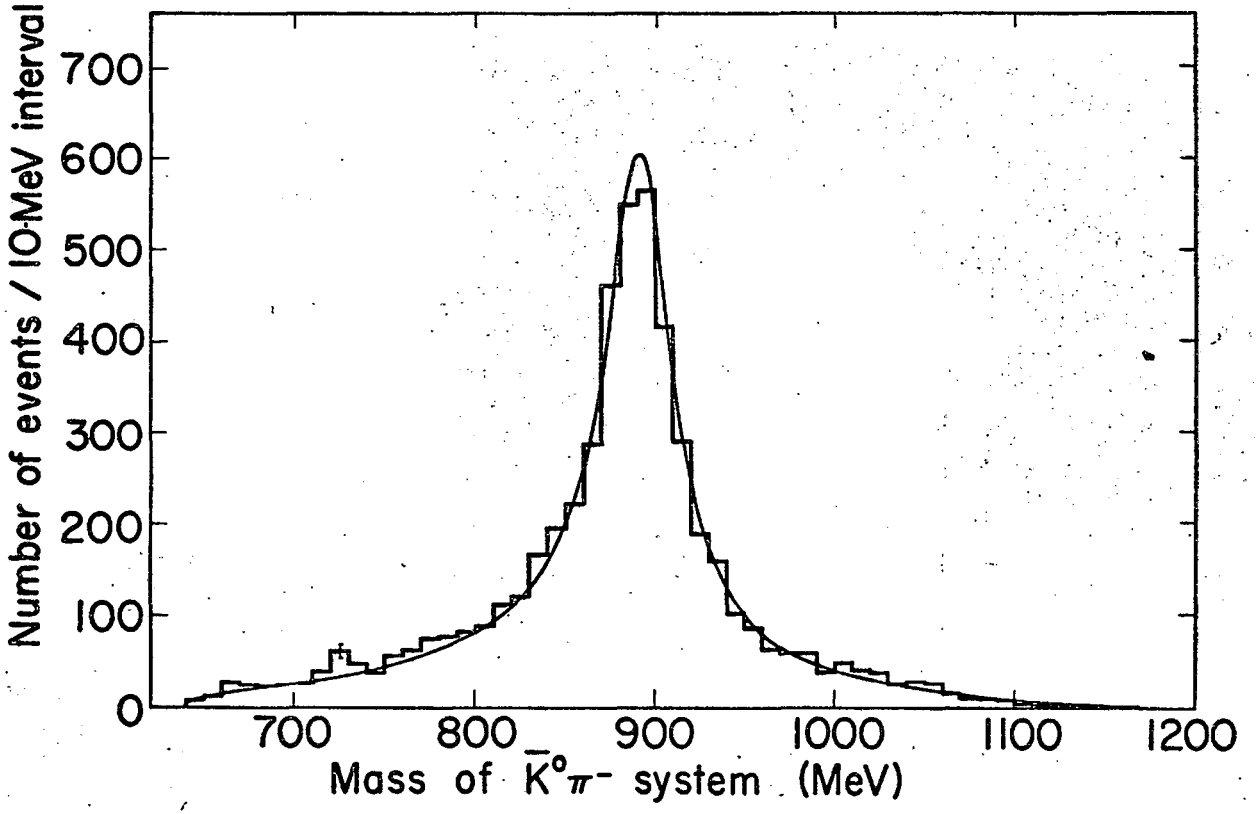

MUB-2272

Fig. 2

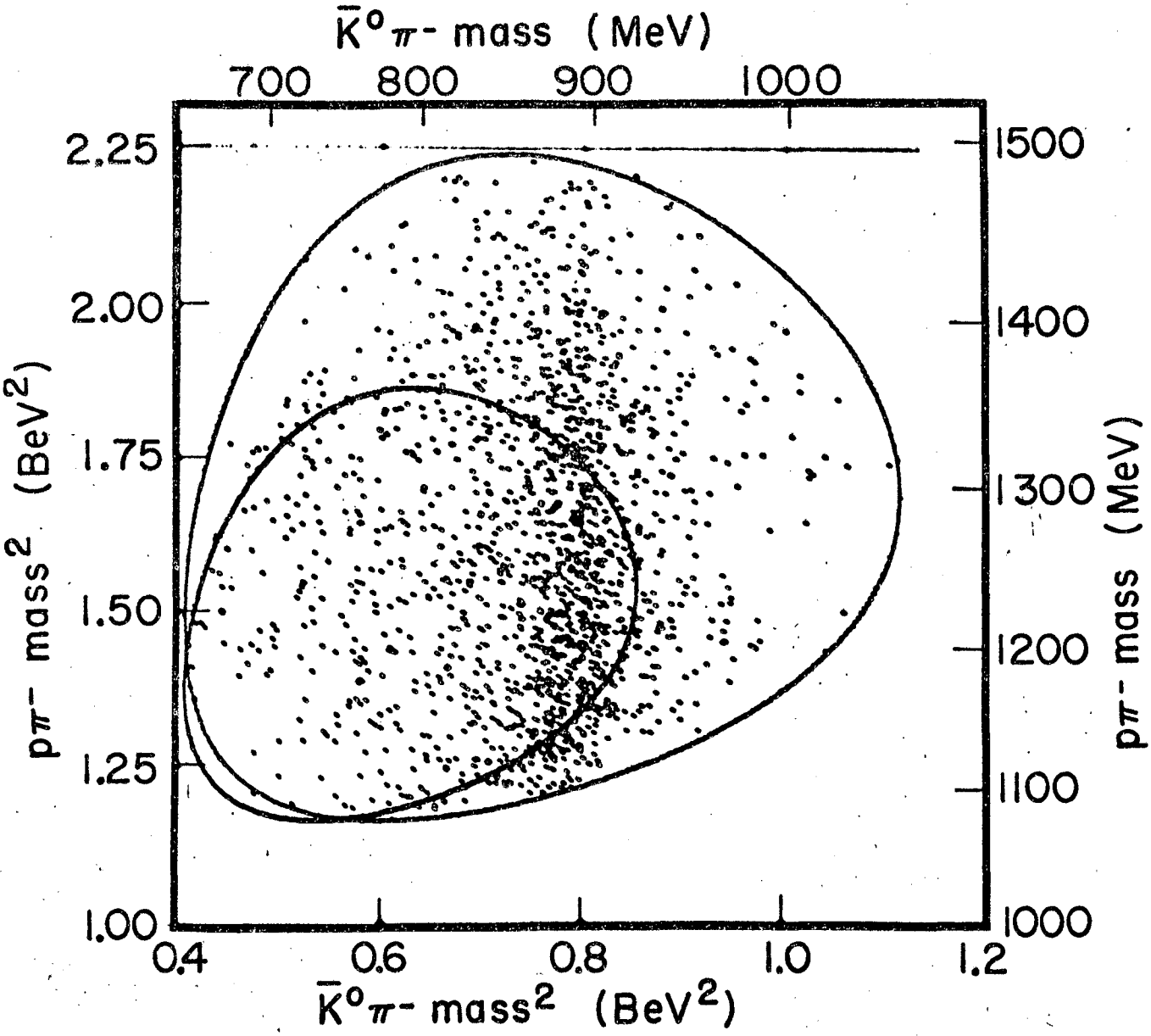

MU-32462

Fig. 3

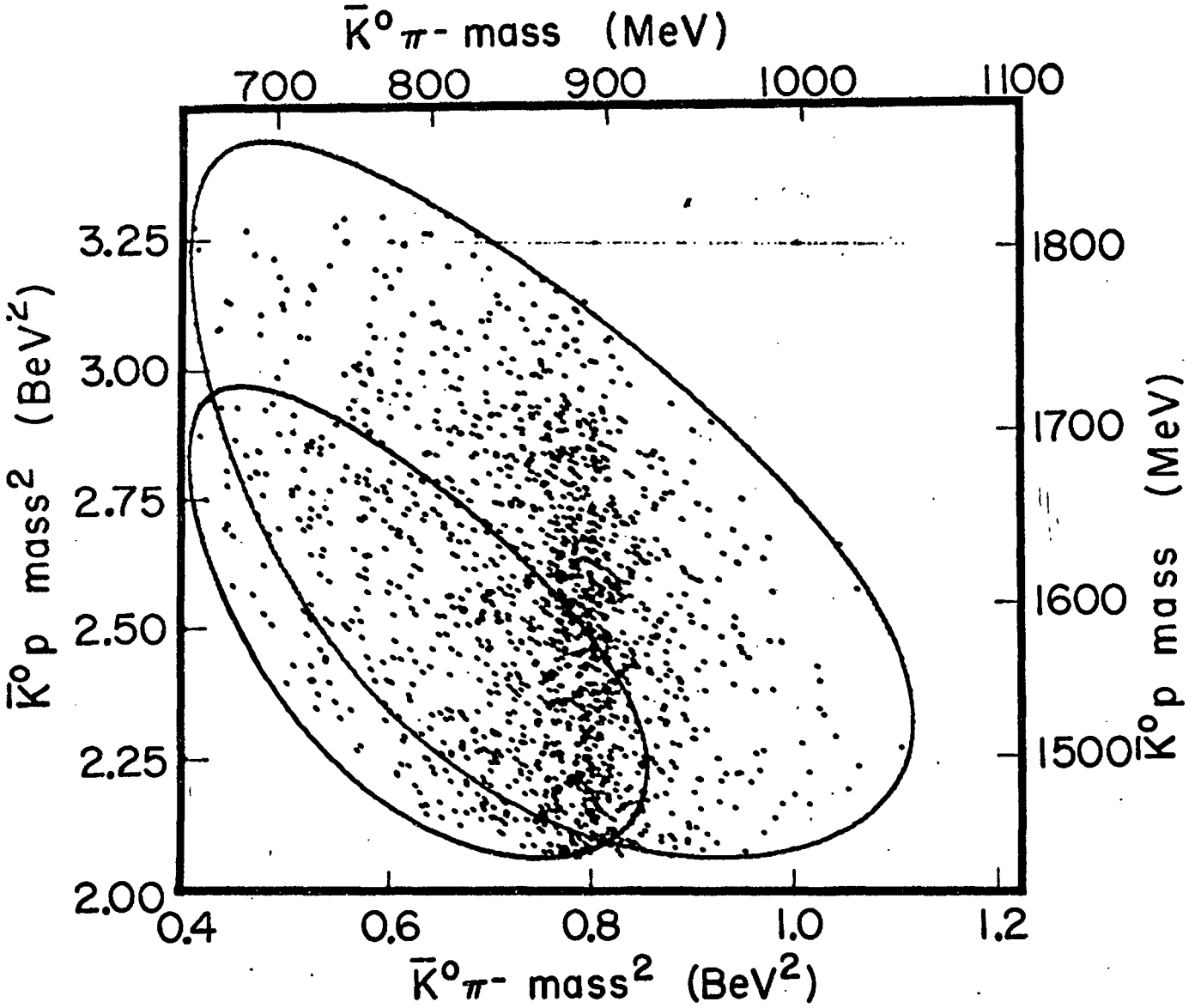
$\bar{K}^0\pi^-$ mass (MeV)
700
800
900
1000
1100
3.25
3.00
2.75
2.50
2.25
2.00
$\bar{K}^0 p$ mass^2 (BeV^2)
1800
1700
1600
1500
$\bar{K}^0 p$ mass (MeV)
0.4
0.6
0.8
1.0
1.2
$\bar{K}^0\pi^-$ mass^2 (BeV^2)
MU-32461

Fig. 4

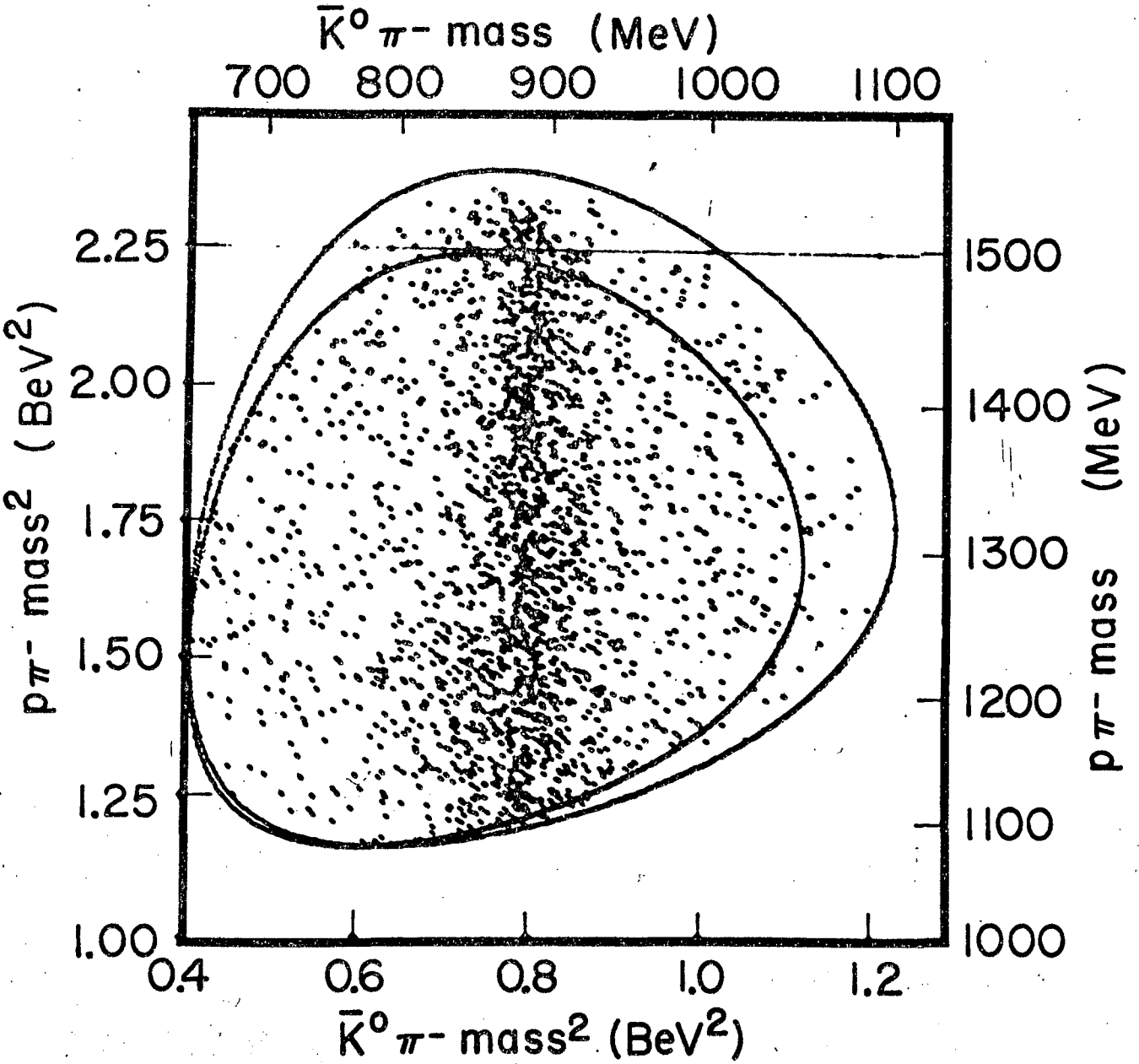

MU-32466

Fig. 5

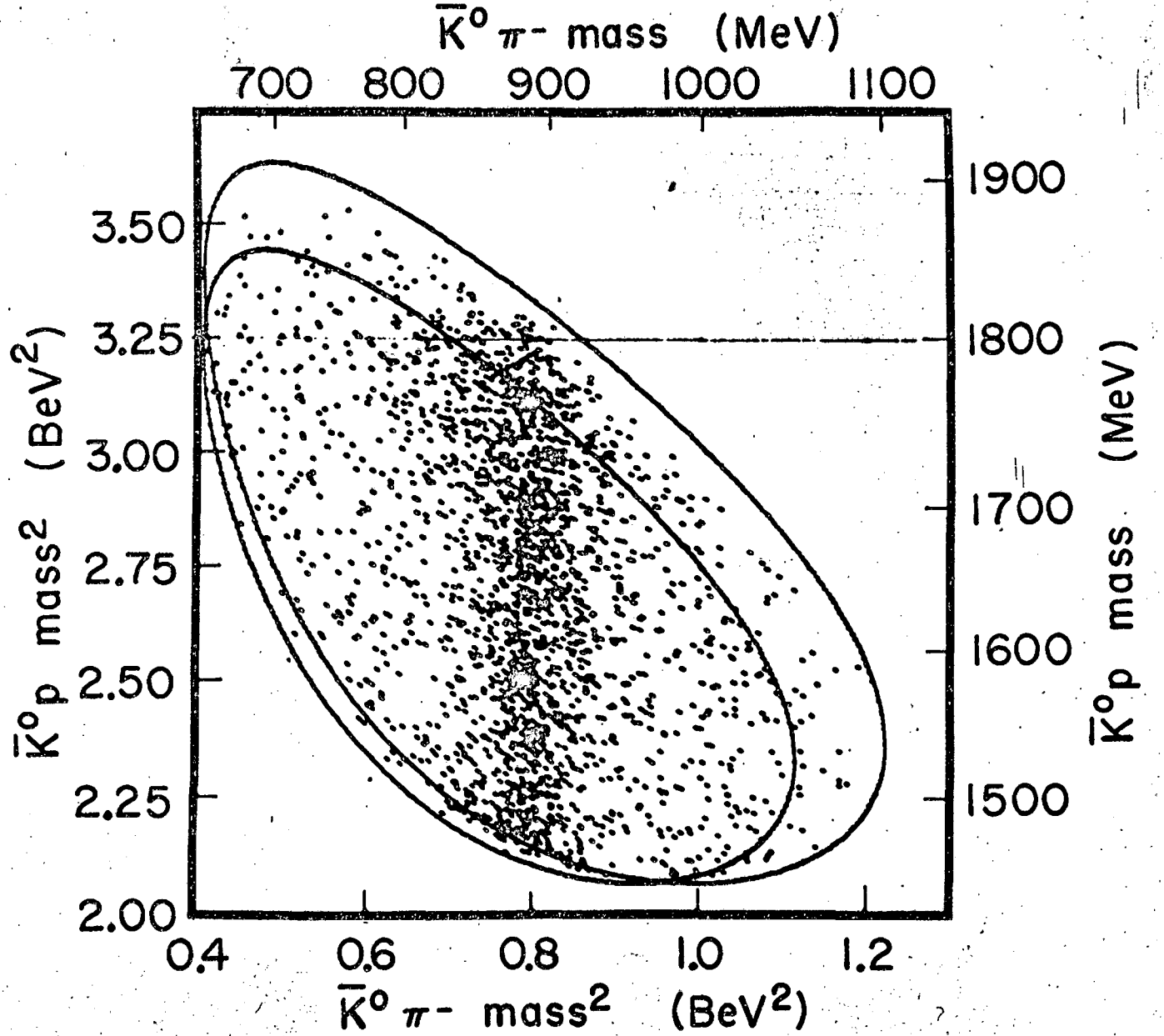
$\bar{K}^0\pi^-$ mass (MeV)
700
800
900
1000
1100
3.50
3.25
3.00
2.75
2.50
2.25
2.00
$\bar{K}^0p$ mass^2 (BeV^2)
1900
1800
1700
1600
1500
$\bar{K}^0p$ mass (MeV)
0.4
0.6
0.8
1.0
1.2
$\bar{K}^0\pi^-$ mass^2 (BeV^2)
MU-32464

Fig. 6

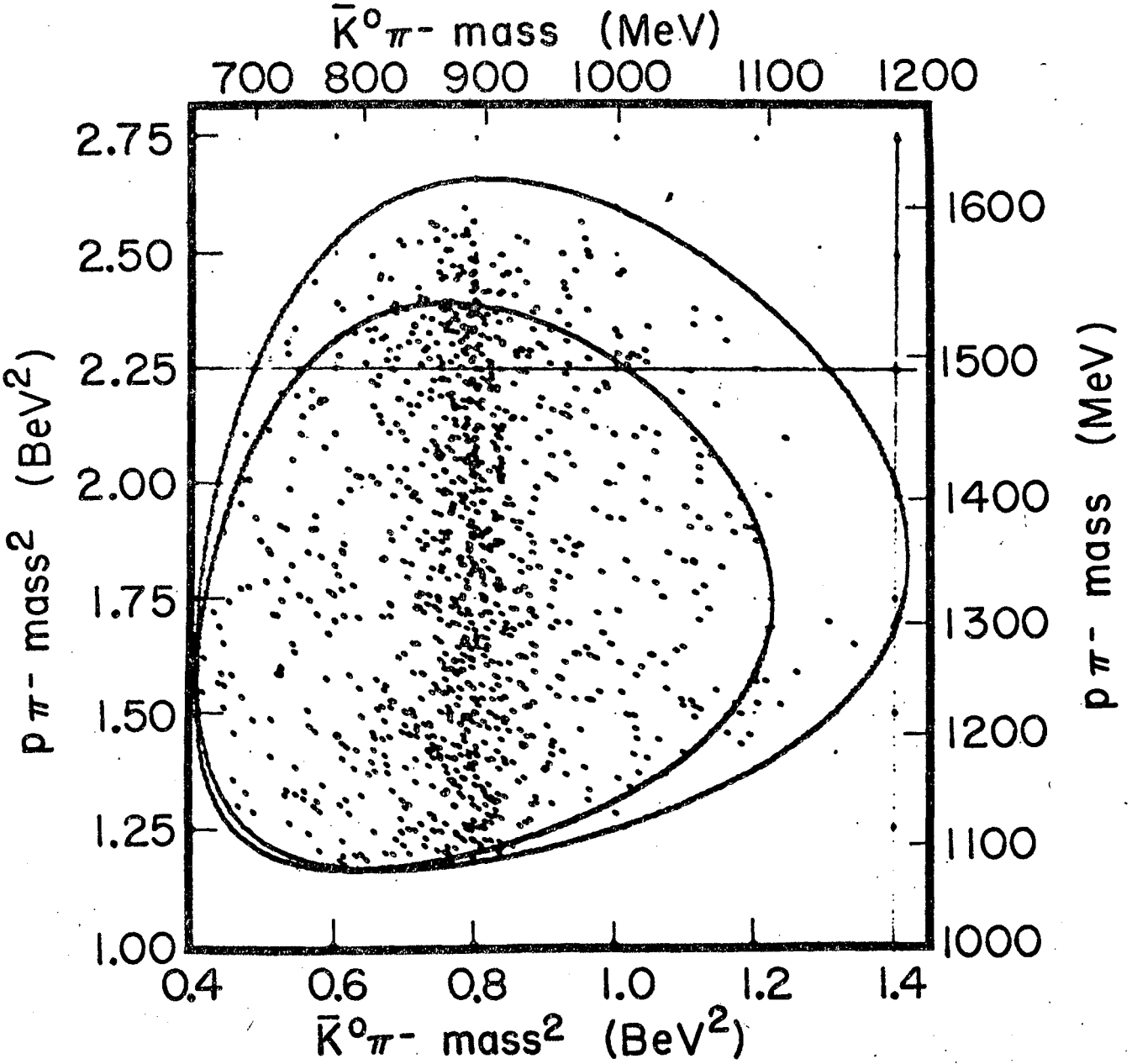
$\bar{K}^0\pi$- mass (MeV)
700 800 900 1000 1100 1200
2.75
2.50
2.25
2.00
1.75
1.50
1.25
1.00
$p\pi$- mass^2 (BeV^2)
1600
1500
1400
1300
1200
1100
1000
$p\pi$- mass (MeV)
0.4 0.6 0.8 1.0 1.2 1.4
$\bar{K}^0\pi$- mass^2 (BeV^2)
MU-32463

Fig. 7

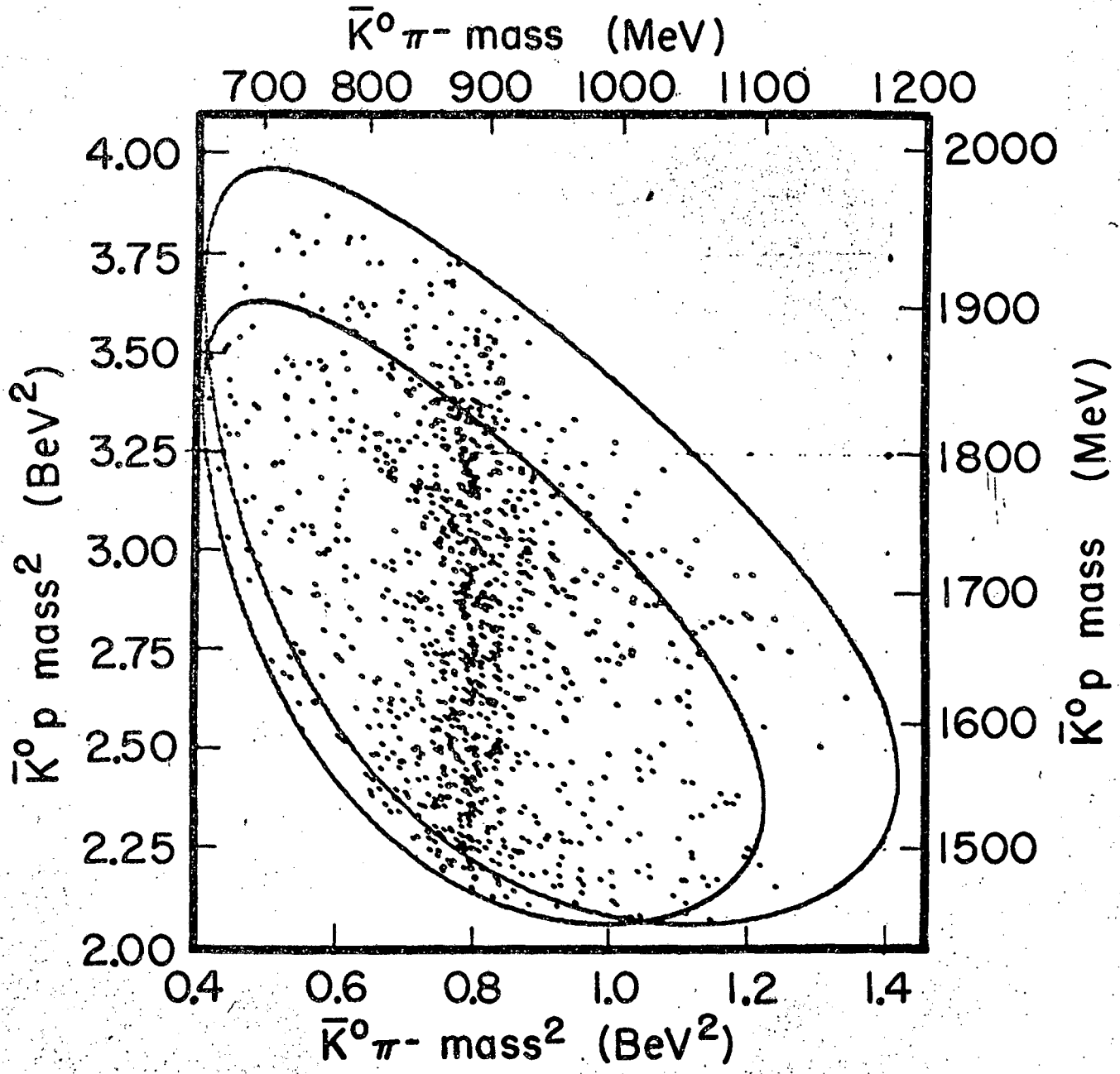
$\bar{K}^0\pi^-$ mass (MeV)
700 800 900 1000 1100 1200
4.00
3.75
3.50
3.25
3.00
2.75
2.50
2.25
2.00
$\bar{K}^0p$ mass^2 (BeV^2)
2000
1900
1800
1700
1600
1500
$\bar{K}^0p$ mass (MeV)
0.4 0.6 0.8 1.0 1.2 1.4
$\bar{K}^0\pi^-$ mass^2 (BeV^2)
MU-32465

Fig. 8

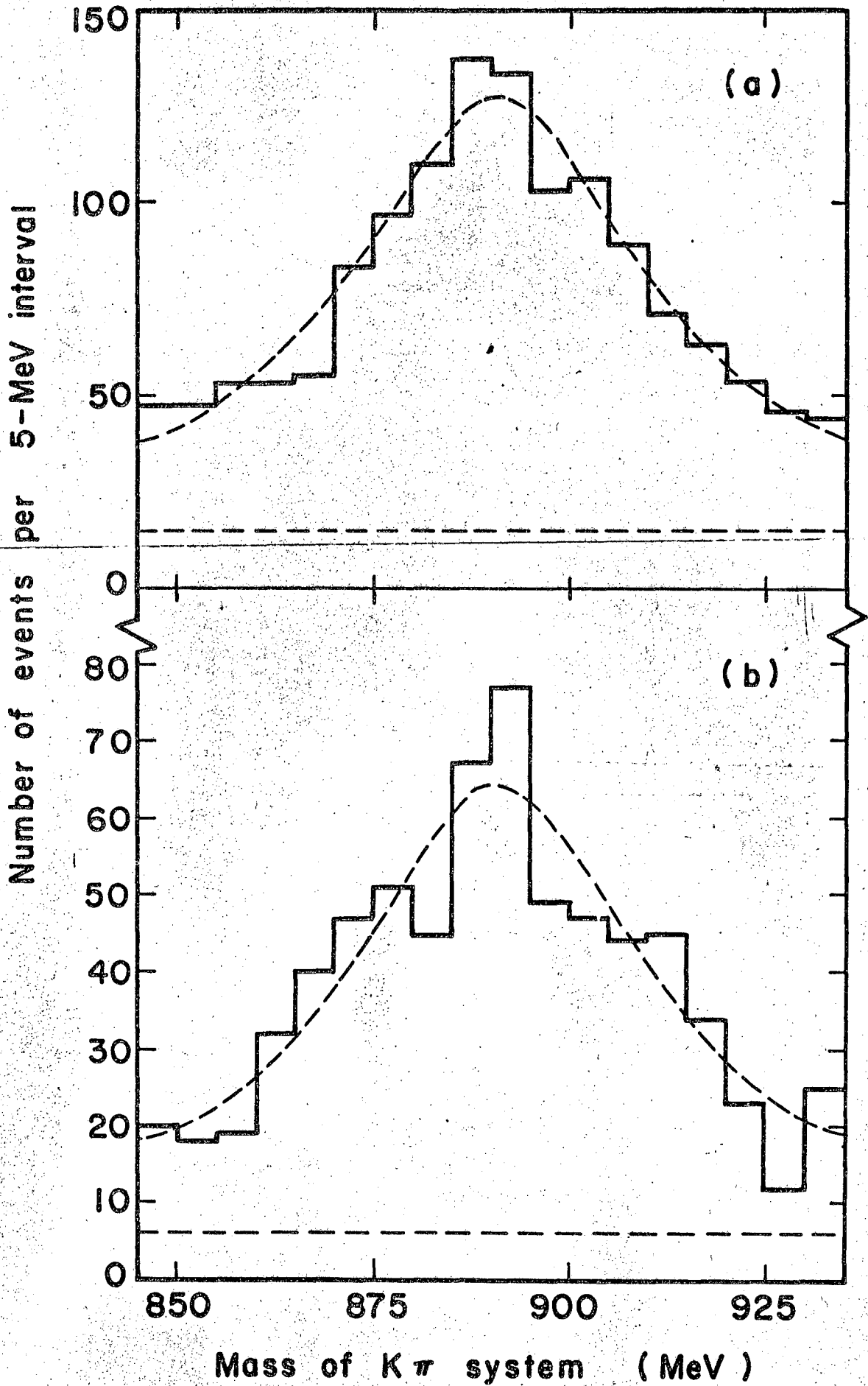

Fig. 9

MU-32636

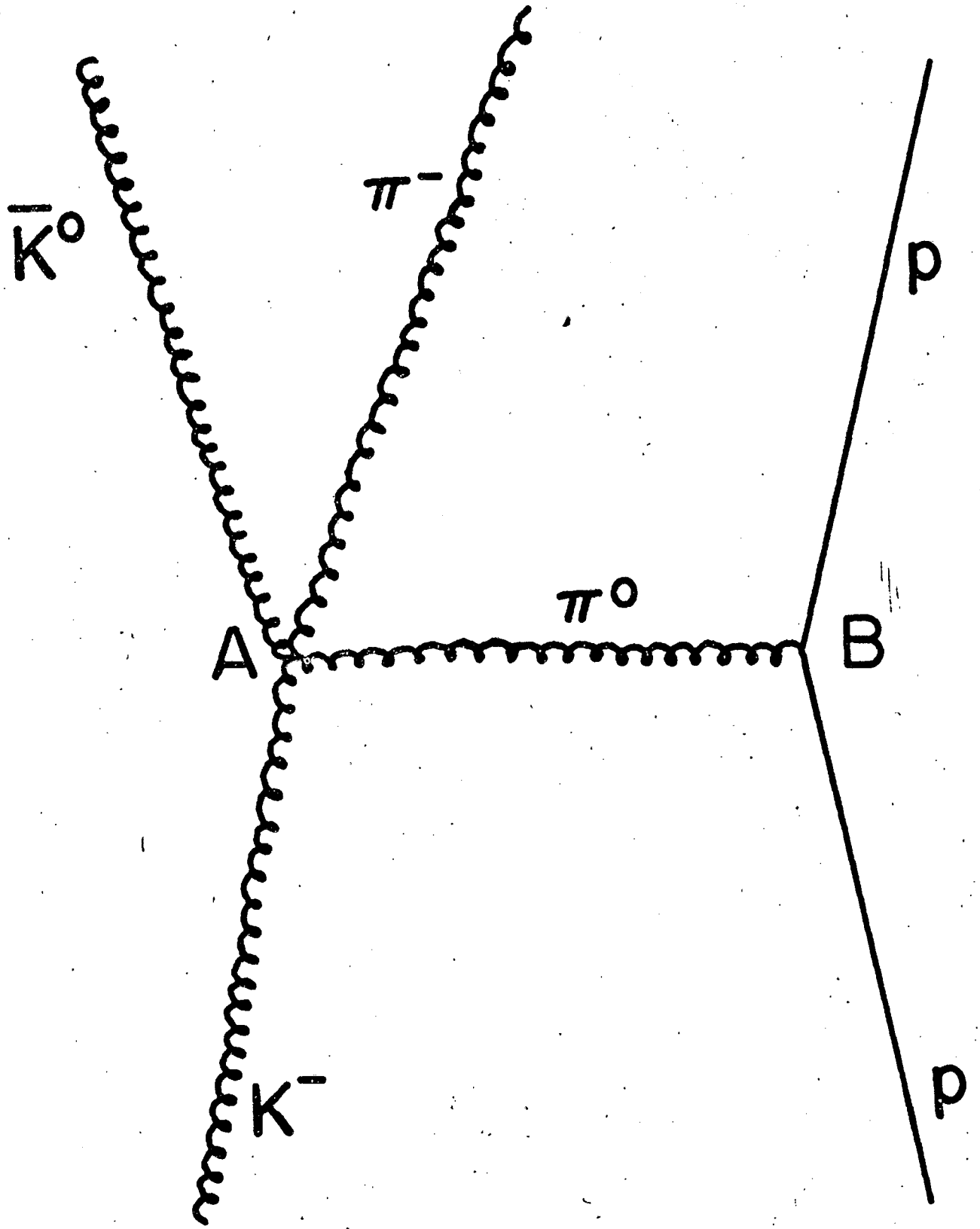

Fig. 10

MU-32833

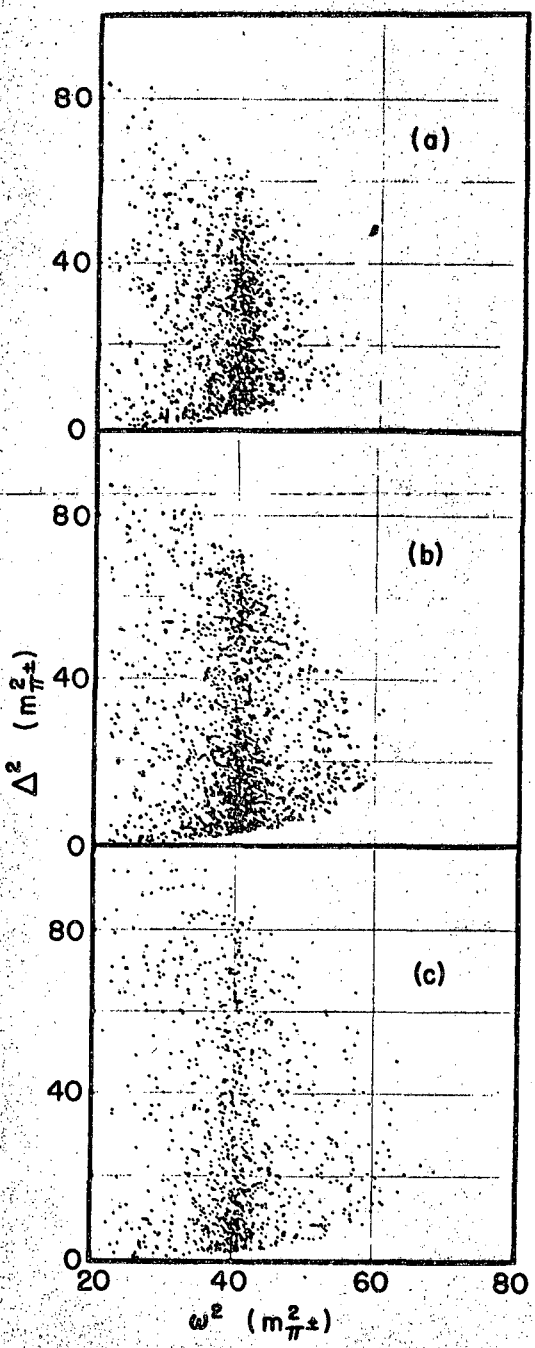
80
40
0
(a)
80
40
0
(b)
80
40
0
(c)
Δ^2 ($m^2_{\pi^\pm}$)
20
40
60
80
ω^2 ($m^2_{\pi^\pm}$)
MUB-2190

Fig. 11

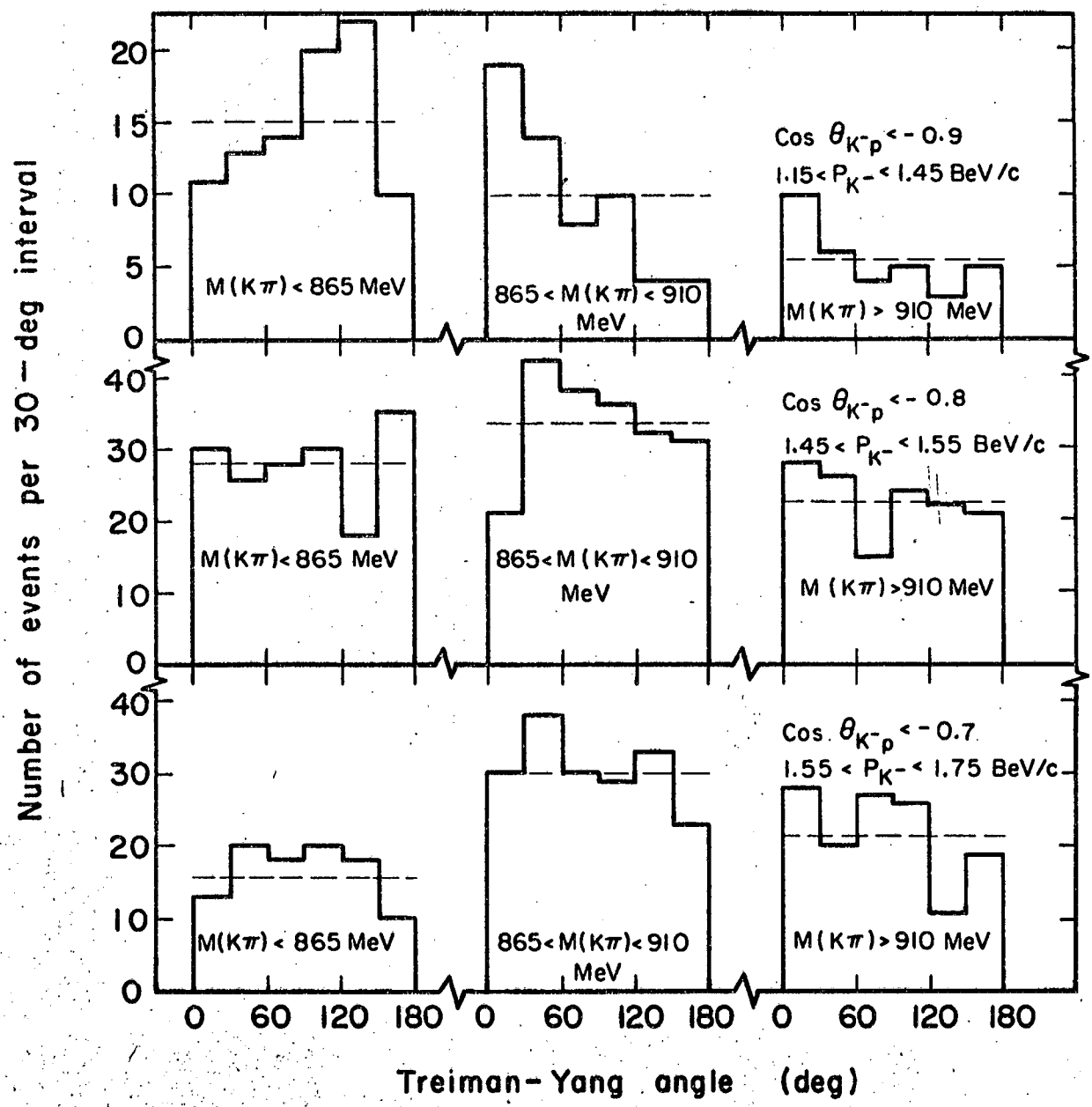

MUB-2235

Fig. 12

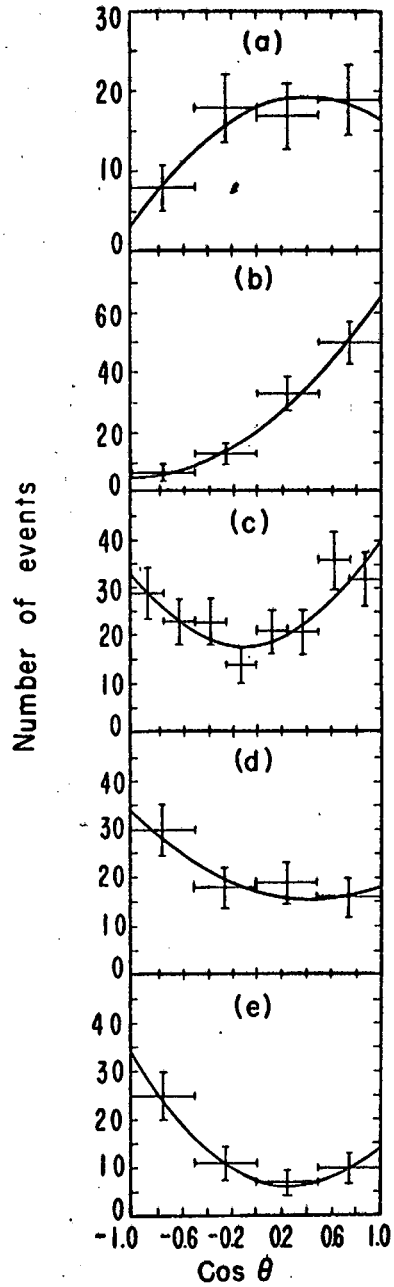

Fig. 13

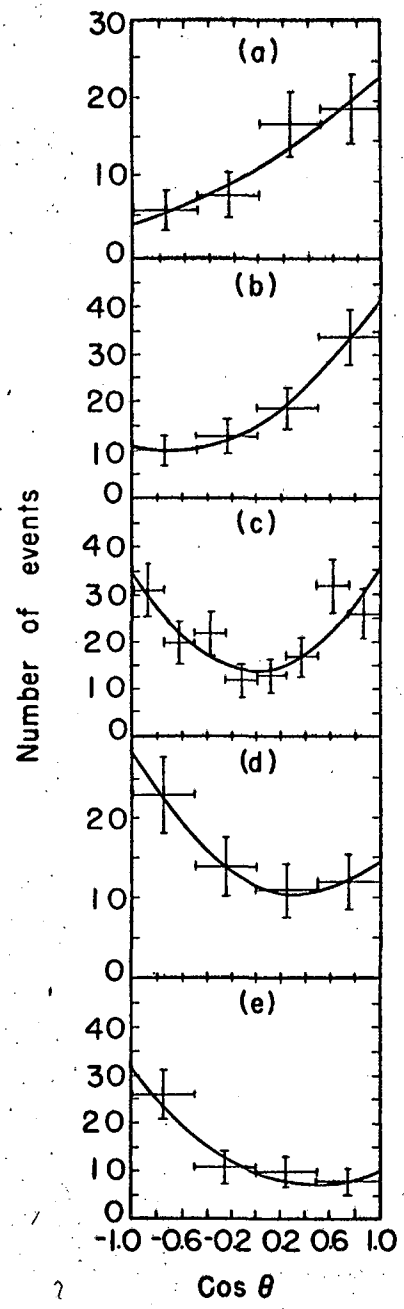

Fig. 14

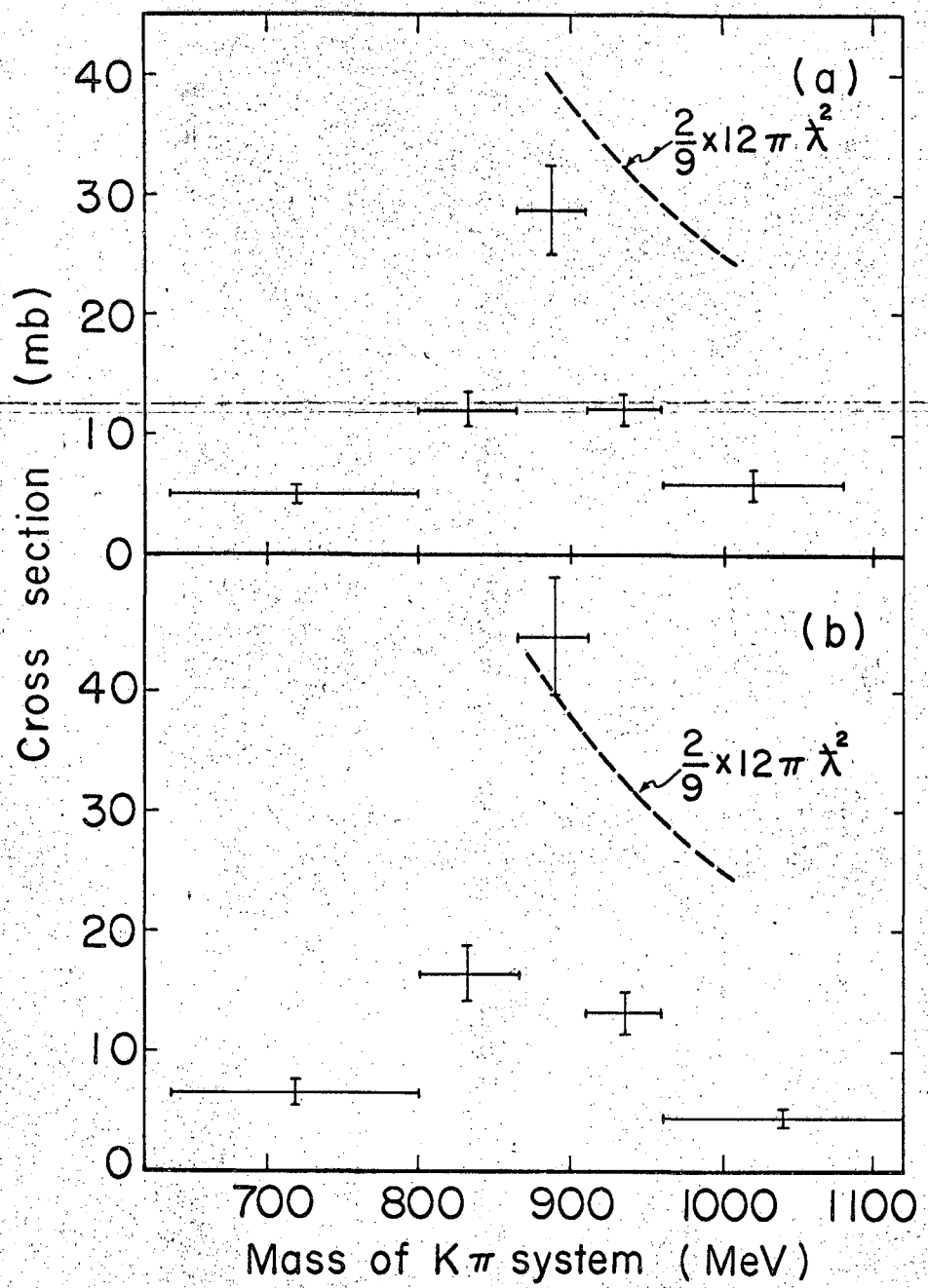

MUB-2220

Fig. 15

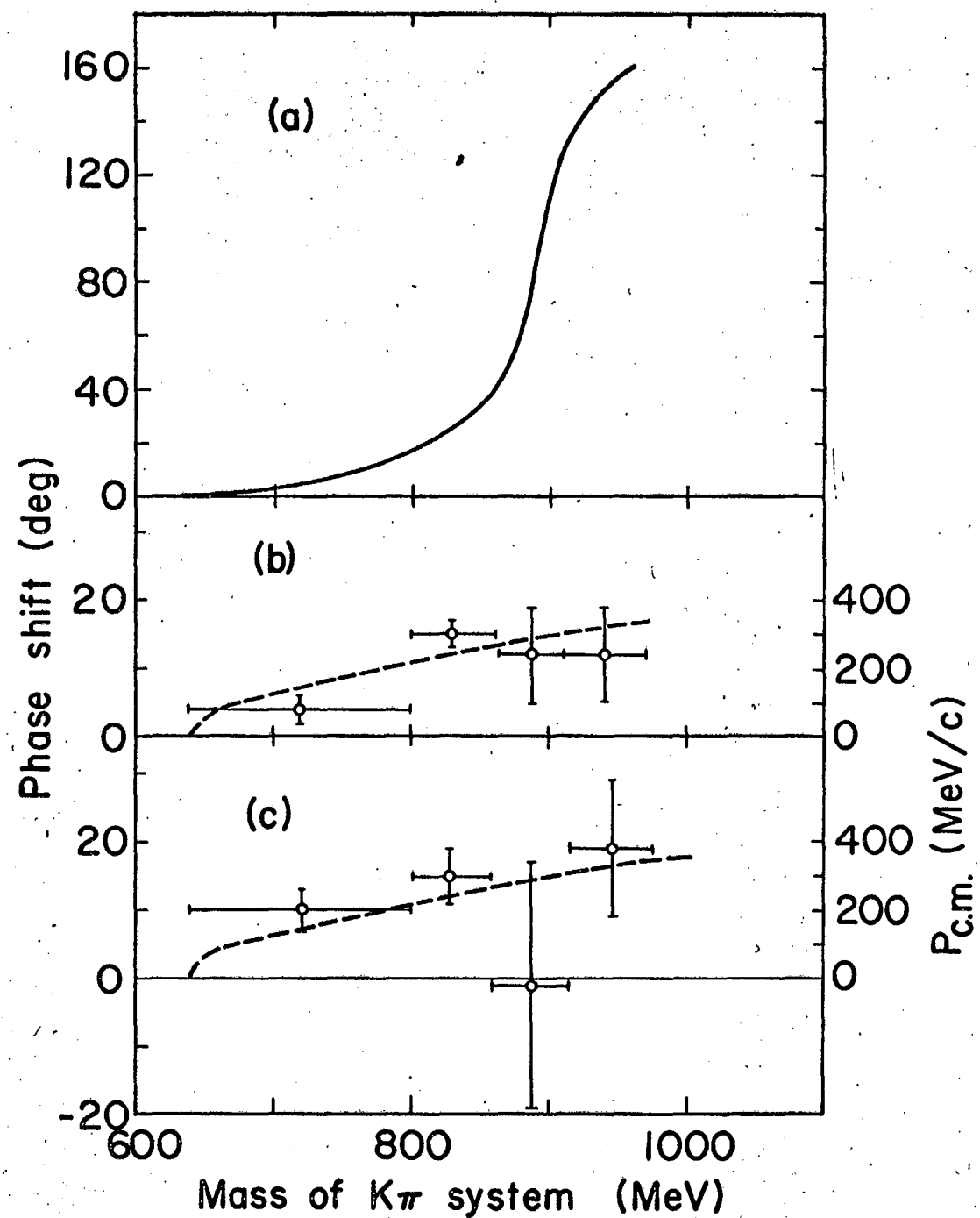

MUB-2274

Fig. 16

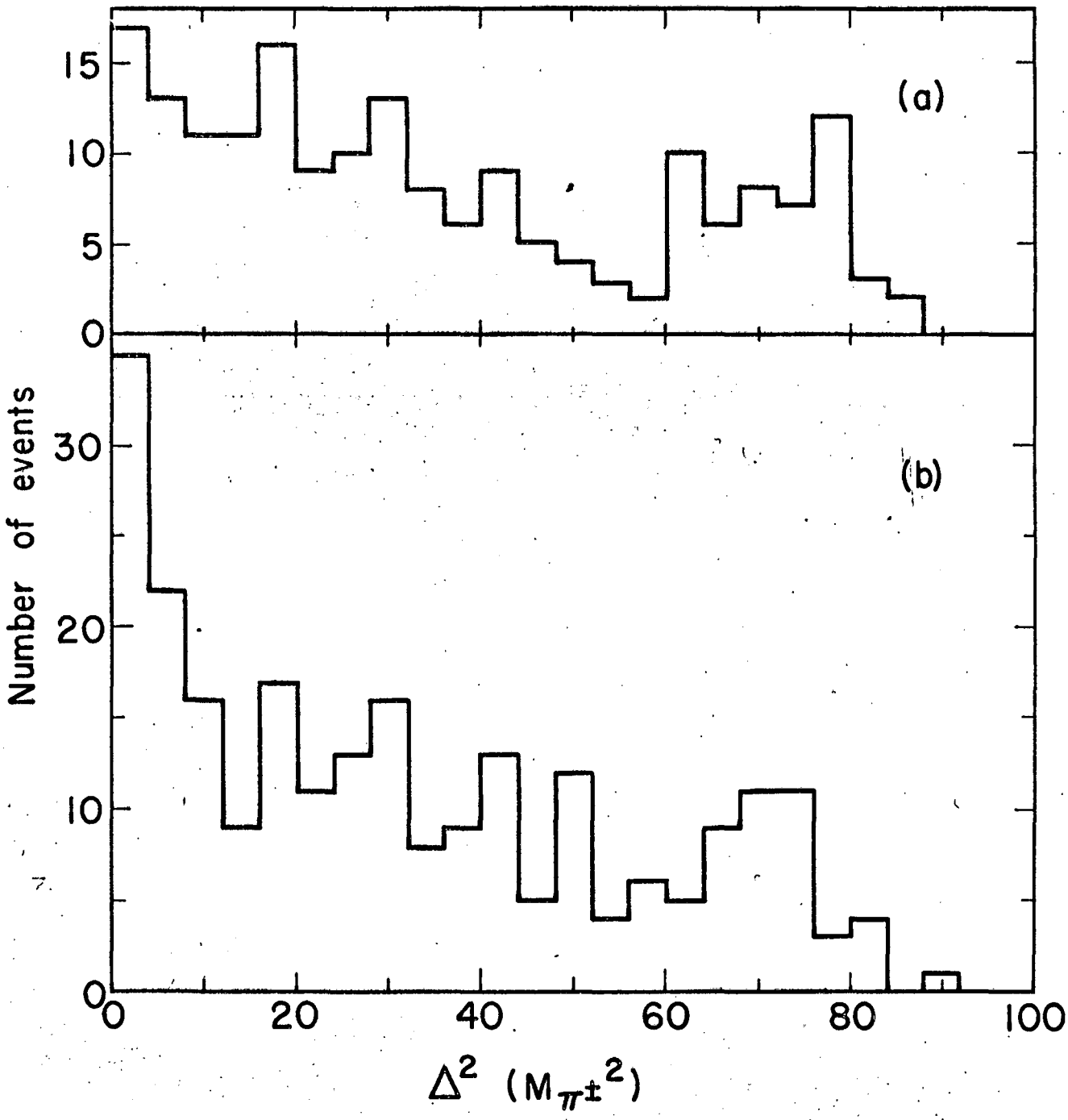

MUB-2273

Fig. 17

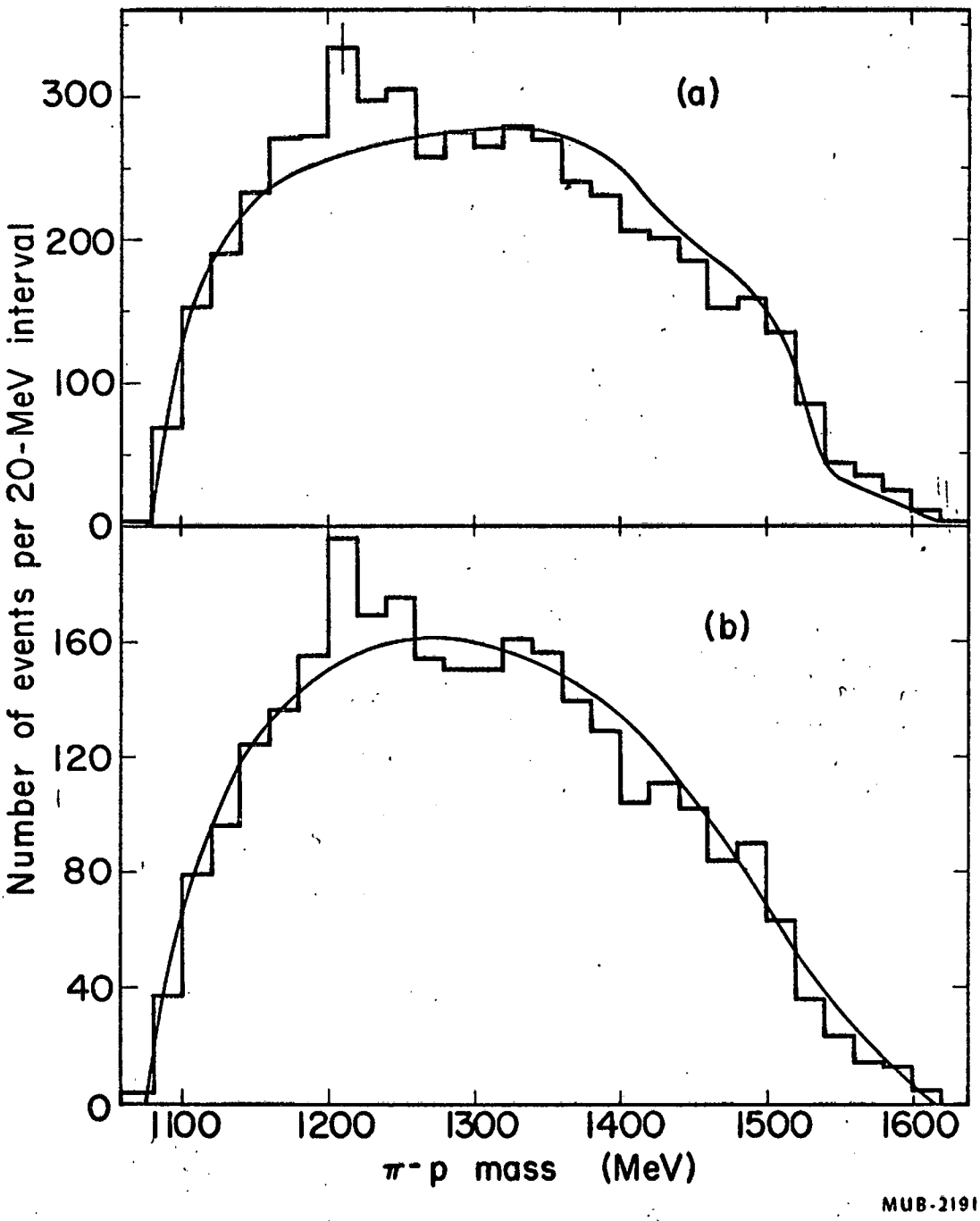
(a)
(b)
300
200
100
0
160
120
80
40
0
Number of events per 20-MeV interval
1100
1200
1300
1400
1500
1600
π⁻p mass (MeV)
MUB-2191

Fig. 18

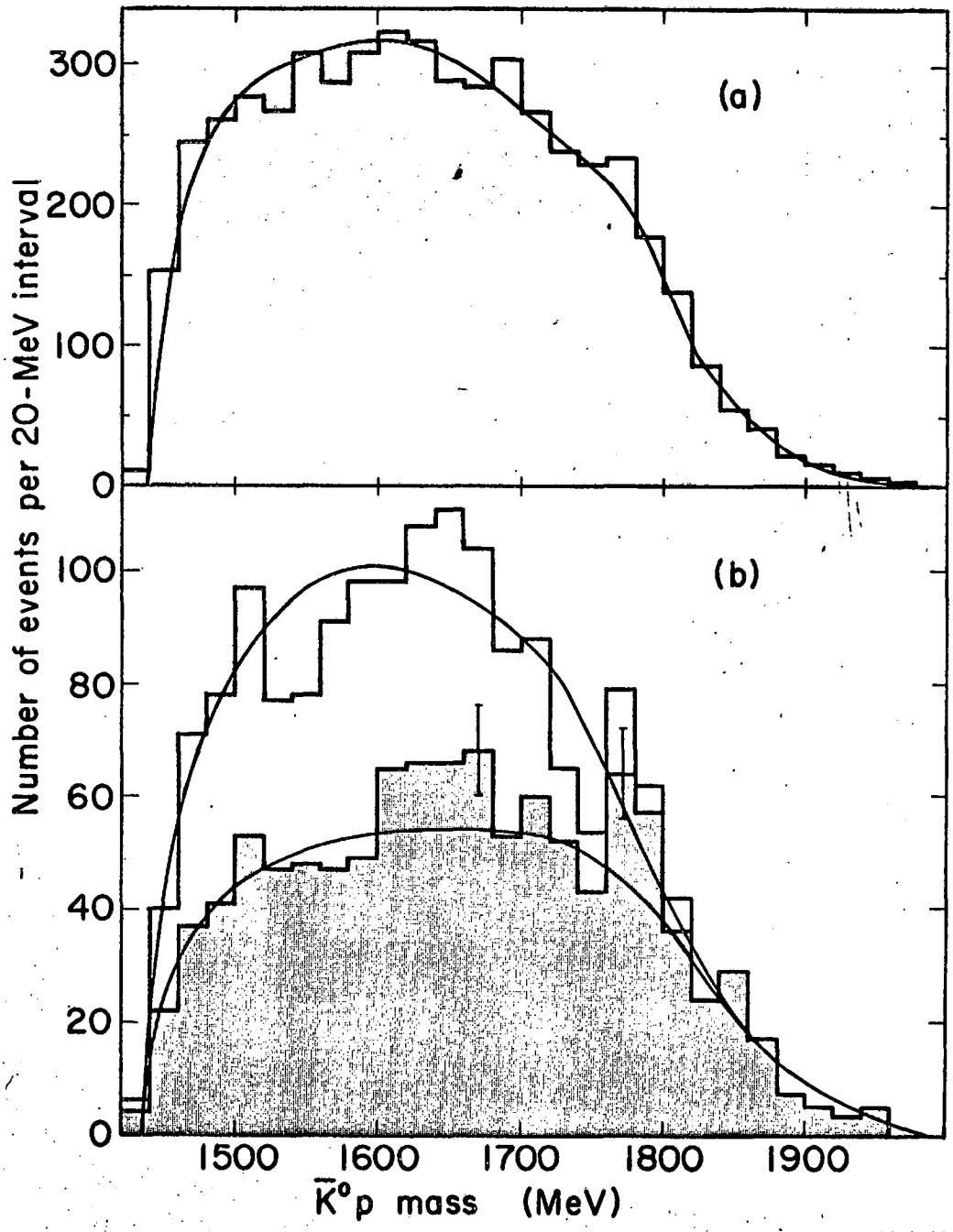
(a)
(b)
Number of events per 20-MeV interval
$\bar{K}^0 p$ mass (MeV)
0
100
200
300
20
40
60
80
100
1500
1600
1700
1800
1900
MUB-2192

Fig. 19

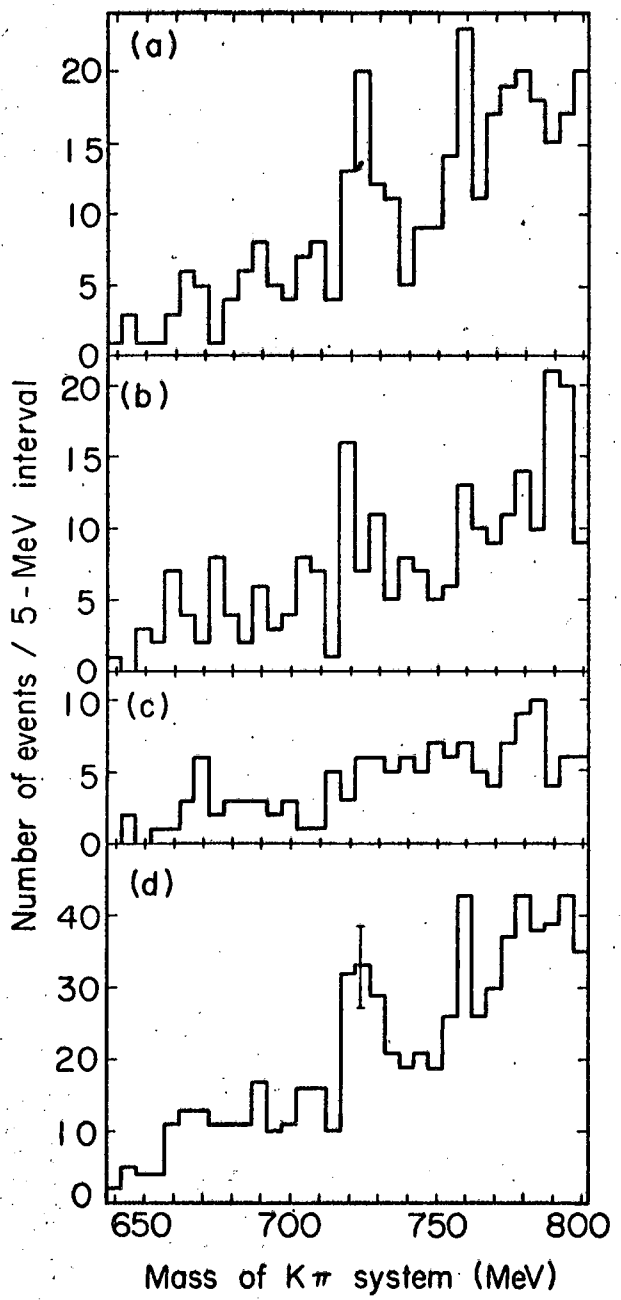
(a)
(b)
(c)
(d)
Number of events / 5-MeV interval
Mass of Kπ system (MeV)
650
700
750
800
MUB-3222

Fig. 20